



## State-of-the-art on catalytic hydrogenolysis of lignin for the production of aromatic chemicals

Chongbo Cheng,<sup>a</sup> Dekui Shen,<sup>\*a</sup> Sai Gu<sup>b</sup> and Kai Hong Luo<sup>c</sup>

Received 00th January 20xx,  
Accepted 00th January 20xx

DOI: 10.1039/x0xx00000x

www.rsc.org/

Solvolytic is one of the promising methods to convert lignin to different kinds of value-added aromatic chemicals in the solvent, sometimes employing catalytic system and hydrogen. The process involving the cracking of the lignin macromolecule and repolymerization of the produced fragments is influenced by the heating method, experimental conditions, presence of catalyst and solvent species. The inter-unit linkages in lignin can be selectively cleaved with addition of the designed catalyst, facilitating the formation of the aromatic compounds. Favorable solvent system could improve the yield of specific aromatic compounds and inhibit the formation of polymerized compounds. This work aims to provide a comprehensive review on lignin hydrogenolysis concerning the effect of catalyst and solvent on the cleavage mechanism of typical inter-unit linkages and the final product distribution. The limitations and forward routes for this area are addressed, in order to emphasize the requirement on understanding the lignin hydrogenolytic depolymerization process for aromatic platform chemicals production.

### 1 Introduction

Today, about ten percent of the global primary energy is provided by biomass (as it is available in quantities more than 10<sup>11</sup> tonnes per year worldwide),<sup>1</sup> which is the fourth major source of energy in the world followed by oil, coal, and natural gas.<sup>2,3</sup> With the depletion of fossil fuels, the fraction of energy and chemicals supplied by biomass can be expected to predominate in the foreseeable future.<sup>4,5</sup> Lignocellulose, the main nonfood component of biomass, consists of cellulose, hemicellulose, and lignin, which acts as the potential feedstock for the production of liquid fuels and value-added chemicals. Although liquid fuels and chemicals obtained from biomass-refinery processes have been already made advancements,<sup>6</sup> the use of lignocellulose as carbon feedstock for the chemical industry that produces higher value bio-based products, ranging from carbon materials to pharmaceutical chemicals, is still in fledging stages.<sup>7-14</sup> As the price of fossil-based fuels goes down, lignocellulose represents a preferable source for producing value-added platform chemicals.<sup>15</sup>

Lignocellulosic biomass composed of semi-crystalline polysaccharide cellulose (38-50%), amorphous multicomponent polysaccharide hemicellulose (23-32%) and amorphous phenylpropanoid polymer lignin (15-25%).<sup>16-18</sup> The conversion of cellulose and hemicellulose with repetitive structural units into biofuels and valuable platform chemicals (e.g. levulinic acid, formic

acid, furfural, gamma-valerolactone and derivatives) has made great progresses.<sup>19-21</sup> However, lignin is the most thermally stable fraction, less than 2% of which can be effectively converted for high-valued chemicals production.<sup>22,23</sup> The reliable technology for the efficient depolymerization of lignin was demanded,<sup>24</sup> due to that it is the unique renewable source for the production of renewable aromatic platform chemicals.<sup>5,12,25-28</sup>

In the past decades, a family of thermochemical methods, such as pyrolysis,<sup>29-33</sup> acidolysis,<sup>34</sup> oxidation,<sup>6,15,35,36</sup> hydrogenolysis<sup>3,4,37-39</sup> and so on, had been developed to convert lignin into aromatic monomers. Syngas or pyrolysis oils can be obtained from pyrolysis and gasification of lignocellulose or lignin.<sup>15</sup> It usually gives higher oxygen content in products mainly including aromatic aldehydes and carboxylic acids by oxidation methods.<sup>40</sup> The yield of aromatic monomers obtained by acidolysis and oxidation methods is relatively low. Comparatively, hydrogenolysis (molecular hydrogen and hydrogen-donor solvent which generates or transfers hydrogen in situ to an acceptor) may be the most promising technology for lignin depolymerization, due to the relatively higher yield of aromatic monomers.<sup>18</sup> Catalytic technologies have attracted more and more attentions, mainly ascribed to the high yield and selectivity of specific aromatic products. The separation and purification processes after lignin depolymerization process are also important in order to meet the final products requirements.<sup>41</sup>

In this work, the structural characteristics of lignin from different sources were briefly introduced together with the lignin-derived model compounds that mirror representative linkages. Catalytic hydrogenolysis of lignin and its model compounds is intensively discussed in this work, concerning the influence of catalyst and solvent on the product distribution, as well as cracking mechanism of the typical inter-unit linkages. Finally, novel technologies

Key lab of Thermal Energy Conversion and Control of MoE, Southeast University, Nanjing 210096, China. E-mail: 101011398@seu.edu.cn

Department of Chemical and Process Engineering, Faculty of Engineering and Physical Sciences, University of Surrey, GU2 7XH, UK

Department of Mechanical Engineering, University College London, London WC1E 7JE, UK

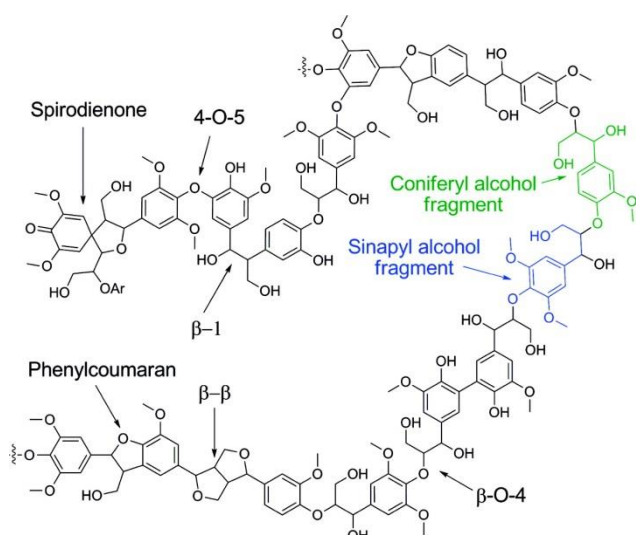


Fig. 1 Schematic depiction of a hardwood lignin structure, showing various linkages, adapted from 4.

including the two-step LDP (lignin depolymerization) and the methods to avoid repolymerization are presented for emphasizing the limitations during the lignin depolymerization process.

## 2 Chemical structure of lignin

Lignin in the outmost layer behaving like a resin which combines the lignocellulose matrix along while lignin in the cell walls offers strength and rigidity through cross-linking with hemicellulose and cellulose microfibrils.<sup>42</sup> In addition, lignin provides several distinct features such as resistance to corrosion and biological attacks, ultraviolet absorption, as well as water impermeability.<sup>24</sup> Lignin, which exhibits a complex cross-linked amorphous structure, is mainly consisted of three basic phenylpropane units: sinapyl (3,5-dimethoxy-4-hydroxycinnamyl), coniferyl (3-methoxy-4-hydroxycinnamyl) as well as *p*-coumaryl (4-hydroxycinnamyl) alcohols, linked by C-O and C-C bonds.<sup>43, 44</sup> The coniferyl alcohol units contain a single methoxy group while the syringol alcohol units contain two methoxy groups, and *p*-coumaryl alcohol units lack methoxy groups on the aromatic ring (Fig. 1). These three units (C9 units) are commonly termed as syringyl (S), guaiacyl (G), and *p*-hydroxyphenyl (H) units, respectively.<sup>45</sup> Both lignin content of biomass and the ratio of these C9 units are substantially influenced by the kinds of plants and the botanical types and even between trees and the morphological parts of the tree. The lignin content of biomass by weight increases with the following order: grasses < hardwood < softwood.<sup>3</sup> More than 95% of coniferyl alcohol units constitute softwood lignin, while almost the same amounts of coniferyl alcohol units and sinapyl alcohol units are estimated to be in hardwood lignin.<sup>15</sup>

Lignin monolignols are mainly linked via C-O or C-C linkages. Generally, more than 2/3 of the amount linkages are C-O linkages, whereas the other linkages are C-C linkages.<sup>3, 46</sup> To classify the various kinds of linkages between two lignin monolignols, the carbon atoms in the aliphatic side chains of lignin monolignols are termed as  $\alpha$ ,  $\beta$ , and  $\gamma$  with those in the aromatic rings are numbered

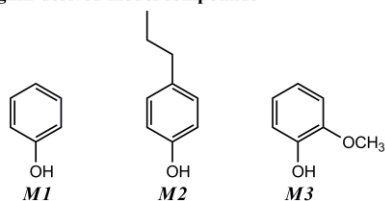
from 1 to 6. Coupling is generally favored at the  $\beta$ -position of the monolignol species, resulting in the main linkages between the lignin monolignols are  $\beta$ -O-4 ( $\beta$ -aryl ether),  $\alpha$ -O-4 ( $\alpha$ -aryl ether),  $\beta$ - $\beta$  (resinol), and  $\beta$ -5 (phenylcoumaran).<sup>37, 47-49</sup> The most frequent coupling linkages in the lignin are  $\beta$ -O-4 bonds, accounting approximately 45 to 48 percent in native lignin.<sup>50, 51</sup> The other linkages involve 5-5 (biphenyl), 4-O-5 (diaryl ether),  $\alpha$ -O- $\gamma$  (aliphatic ether) and  $\beta$ -1 (spirodienone).<sup>4</sup> A schematic depiction of a hardwood lignin involving these linkages is given in Fig. 1. The proportions of these linkages and the functional groups in lignin vary significantly for different plants.<sup>37, 52, 53</sup> Hardwood lignin comprises about 1.5 times more  $\beta$ -O-4 linkages than that of softwood. Additionally, varieties of functional groups such as methoxyl, phenolic hydroxyl, aliphatic hydroxyl, benzyl alcohol, non-cyclic benzyl ether and carbonyl groups in the lignin structure lead to all kinds of reactivity of lignin in lignin depolymerization process.<sup>24</sup>

An important step in biorefinery process is the pretreatment of lignocellulosic biomass. Because of the complex structure of the plant cell walls and the high crystallinity of cellulose, efficient separation of its components is a major challenge. The structure of the extracted lignin is influenced by the separation process leading to significant structural changes.<sup>4</sup> Thus, the behavior of the extracted lignin is substantially different, affecting the distribution of aromatic chemicals obtained from lignin.<sup>54</sup> The high ratio of condensed structures and short side chains in residue lignin will give rise to barriers to lignin depolymerization.<sup>55</sup> Current and emerging isolation methods need to be discussed concerning the characteristics of the extracted lignin as far as its potential for further biorefinery. More information on the lignin structure changes from the isolation methods is comprehensively discussed in other references.<sup>15</sup>

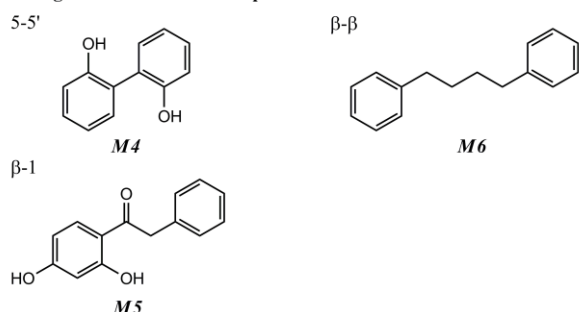
Because of the complex structure in different lignin feedstocks, most of lignin depolymerization researches are performed by using lignin-derived model compounds which mirror the characteristic linkages in lignin. Researches using lignin-derived model compounds gave the better understanding of the cracking mechanism of the nominated linkages. Mostly reported lignin-derived model compounds representing the specific linkages are shown in Fig. 2, cracking of which would be discussed in the section 4.  $\beta$ -O-4 linkage contained model compounds,<sup>56</sup>  $\beta$ -5 linkage contained model compounds,<sup>57</sup>  $\beta$ -1 linkage contained model compounds<sup>58, 59</sup> and  $\beta$ - $\beta$  linkage contained model compounds<sup>60</sup> can be synthesized. Complex lignin-related model compound is required to be synthesized for representing more chemical information in a real lignin sample.<sup>57, 61</sup> Although depolymerization of lignin-related model compounds is considered as one of the accepted methods to understand the cracking mechanism of inter-unit linkages in lignin, the relationship between the depolymerization of lignin and that of its model compounds needs to be specified for optimal selection of catalyst and solvent in the hydrogenolysis system.

The depolymerization of lignin to the specific chemicals is very challenging because of complicated inter-unit linkages in lignin. The process requires severe conditions to crack linkages, meanwhile, the inevitable repolymerization of the fragments leads to the formation of the undegradable products. Heterogeneous catalyst is considered to be difficult to attack the linkages of lignin due to the steric

## Lignin-derived model compounds



## C-C linkage contained model compounds



## C-O linkage contained model compounds

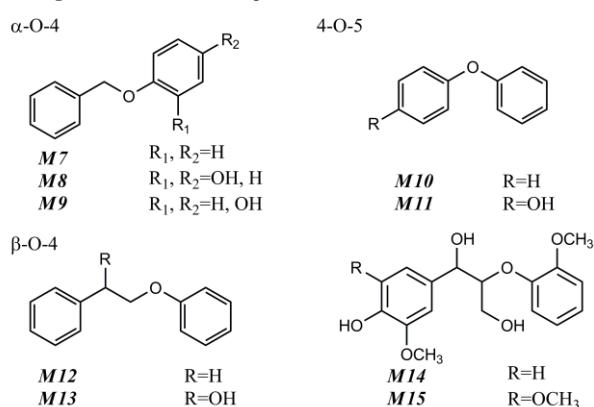


Fig. 2 List of some lignin-related model compounds.

hindrance from the lignin amorphous backbone, resulting in a low selectivity of the aromatic compounds.<sup>57</sup> Homogeneous catalyst can access to the linkages of lignin easily, which is possibly subjected to the decomposition in the solvent system and difficult to be separated from the products.<sup>62</sup>

### 3 Hydrogenolysis of lignin

Hydrogenolysis takes place between hydrogen or a hydrogen-donor reactant and a target compound, is a reductive process. The reaction generally takes place with supported metal catalysts (Pt, Ru, Rh, Pd, Ni etc.). It's a popular and efficient method for cracking the C-O linkages especially beta-O-4 linkages in lignin and for producing aromatic platform chemicals from lignin. Harsh reaction conditions will result in unwanted concurrent cracking of aliphatic ether bonds and saturation of arene rings. The products of hydrogenolysis are phenols, cyclic alcohols and cycloalkanes. The studies on hydrogenolysis of raw lignin samples (organosolv lignin, kraft lignin, soda lignin, etc.) into aromatic compounds are summarized in Table 1.

#### 3.1 Effects of catalysts

Catalyst either homogeneous or heterogeneous is essential for efficient and selective depolymerization of lignin. Comparatively, hydrogenolysis with the addition of heterogeneous catalyst (e.g., metal catalysts, bifunctional catalysts) was mostly reported in the literature.<sup>3</sup>

##### 3.1.1 Homogeneous catalytic system

The depolymerization of wheat straw alkali lignin with phenol as the hydrogen-donor solvent over H<sub>2</sub>SO<sub>4</sub> catalyst was studied (Table 1, entry 1).<sup>63</sup> By comparing tradition heating method, microwave irradiation enhanced the cleavage of C-C bonds (such as an extra 29 % of C<sub>aryl</sub>-C<sub>α</sub> bond cleavage), promoting the yield of monophenolic compounds from 0.92 % to 13.61 %. The solid catalysts such as zeolite (Al<sub>2</sub>(SiO<sub>4</sub>)<sub>3</sub>, Al<sub>2</sub>O<sub>3</sub>) and iron-based catalyst (FeS) have been employed in lignin depolymerization. However, the highest yield of the monophenolic compounds was obtained with H<sub>2</sub>SO<sub>4</sub> as the catalyst.

The hydrogenolysis of aromatic C-O bonds in alkyl aryl and diaryl ethers that form exclusively arenes and alcohols was reported by Sergeev and Hartwig.<sup>88, 89</sup> Hydrogenolysis of the alpha-O-4 lignin model compound with 5 mol % of the Ni-SIPr (soluble nickel carbene complex) catalyst at 80 °C in *m*-xylene and NaO<sup>t</sup>Bu could give the similar production of 3,4-dimethoxytoluene and 2-methoxyphenol. Saturation of aromatic rings was inhibited. With the help of strong base NaO<sup>t</sup>Bu, the formation of anionic nickel complexes was more helpful for cracking the ether bonds or for the coordinated dihydrogen activation. Homogeneous catalysts expressed good performance in chemoselectivity of bond cleavage but need to be further developed in hydrogenolysis of the raw lignin.

##### 3.1.2 Heterogeneous catalytic system

#### Monometallic catalyst

Noble metal catalysts (Pd, Pt, Ru, Rh, etc.) have outstanding catalytic performance in hydrogenolysis process. Hydrogenolysis of organosolv switchgrass lignin to yield phenolic monomers with Pt/C catalyst in ethanol solvent was reported.<sup>64</sup> The least amount of char and the highest proportion of lower molecular weight liquid products with improved H/C and O/C molar ratios were obtained over formic acid and Pt/C catalyst. 21 wt% of *p*-propylguaiacol was obtained after 4h of reaction at 350 °C (Table 1, entry 2). A similar work was reported with the use of Ru/C catalyst. The catalytic conversion of Alcell (organosolv) lignin to alkylphenolics, ketones and aromatics over Ru/C catalyst was reported.<sup>65</sup> 71.2 % yield of oil with 0.09 O/C ratio involving some valuable chemicals such as alkylphenolics (6%), ketones (14%) and aromatics (10.5%) was obtained in iso-propanol/formic acid mixtures (1:1 mass ratio) at 400 °C (Table 1, entry 3). Four lignins (ionic liquid-based mixed organic electrolytes extracted/enzymatic hydrolytic lignins (ILOE-EL/ILOE-EHL) and alkaline twin-screw extrusion extracted/enzymatic hydrolytic lignins (ATSE-EL/ATSE-EHL)) were depolymerized on Pd/C catalyst.<sup>54</sup> The extracted lignin presents much great activity for hydrogenolysis. After 2h reaction at 235 °C in methanol, the overall bio-oil yields of 61.7 and 57.9 wt% could be obtained from ATSE-EL and ILOE-EL,

Table 1 Summary of the hydrogenolysis of raw lignin materials

Entry	Feedstock	Conditions	Solvent	Catalyst	Products	Yield	Ref.
1	Wheat straw alkali lignin	300W, 120 °C, 40 min	Hydrogen donor: phenol; Ethylene glycol	H <sub>2</sub> SO <sub>4</sub>	Monophenolic compounds	15.77 wt %	63
2	Switchgrass lignin	350 °C, 1/4/8/20 h	Hydrogen donor: formic acid; Ethanol	Pt/C	Lower molecular weight compounds ( <i>p</i> -propylguaiacol)	21 wt %	64
3	Alcell(Organosolv) lignin	400 °C, 4h	Hydrogen donor: iso-propanol-formic acid; ethanol-formic acid; methanol-formic acid	Ru/C	Bio-oil (alkylphenolics, aromatics)	71 wt % (6 wt%, 11 wt%); 63 wt % (7 wt %, 17 wt %); 68 wt % (11 wt %, 19 wt %)	65
4	Birch sawdust	200 °C, 6 h, 0.1 Mpa Ar	CH <sub>3</sub> OH; i-PrOH; 1,4-Dioxane; Glycerol; Cyclohexane	Ni/C	Aromatic products (propylguaiacol, propylsyringol)	54 % conversion (22 %, 67 %); 27 % conversion (12 %, 37 %); 15 % conversion (none, 6 %); 16 % conversion (16 %, 67 %); <1 % conversion (none, none)	66
5	Organosolv lignin	300 °C, 24h	Hydrogen donor: supercritical methanol	Cu-PMO	Monomeric substituted cyclohexyl derivatives	/	67
6	Wood and cellulosic solids	300-320 °C, 8h, 16-22 MPa	Hydrogen donor: supercritical methanol	Cu-PMO	Aliphatic alcohols and methylated derivatives (C <sub>2</sub> -C <sub>6</sub> species, C <sub>9</sub> -C <sub>12</sub> species)	~85 % conversion (10.0 wt %, 5.8 wt %)	68
7	Organosolv lignin	180 °C, 14h, 4MPa H <sub>2</sub>	Hydrogen donor: supercritical methanol	Cu-PMO	Aromatic products (catechols)	>90 % conversion (63.7 wt %)	69
8	Soda lignin	300/340 °C	Hydrogen donor: supercritical methanol	TiN; NbN; Mo <sub>2</sub> N; W <sub>2</sub> N	Aromatic monomers	19 wt %; 17 wt %; 7 wt %; 3 wt %;	70
9	KL/AL/EL lignin	340/380 °C, 2/6h	Hydrogen donor: formic acid; water	Ru/Al <sub>2</sub> O <sub>3</sub> ; Rh/Al <sub>2</sub> O <sub>3</sub> ; Pd/Al <sub>2</sub> O <sub>3</sub>	Bio-oil	91.5 wt %; 80.5 wt %; 82.9 wt %	71
10	Organosolv olive tree pruning lignin	400W, 140 °C, 30 min	Hydrogen donor: tetralin; formic acid	NiAlSBA-15; PdAlSBA-15; PtAlSBA-15; RuAlSBA-15	Bio-oil	10 wt % (NiAlSBA-15); 30 wt % (NiAlSBA-15)	72
11	Organosolv hydrolyzed lignin	300 °C, 4 h, 1 MPa H <sub>2</sub>	Ethanol	Ni/Al-SBA-15	Aromatic monomers	21.90 wt %	73
12	Spruce lignin	300 °C, 2/4/21h	Hydrogen donor: formic acid; water	Pd and Nafion SAC-13	Phenols (guaiacol, pyrocatechol, resorcinol)	7.7 wt % (2.0 wt %, 3.7 wt %), 2.0 wt %)	74
13	Residue lignin; Recovered insoluble lignin	250 °C, 4 h, 4 MPa H <sub>2</sub>	Water	HY zeolite and Ru/Al <sub>2</sub> O <sub>3</sub>	Hydrocarbon products	22 wt % (Recovered insoluble lignin)	55

14	Pine wood lignin	250 °C, 4 h, 4 MPa H <sub>2</sub>	Water	Ru-Cu/HY	Hydrocarbon products	32 wt %	75
15	Enzymatic corn cob lignin	300 °C, 160 min, 6 MPa H <sub>2</sub>	Dodecane	Ni/ASA	C <sub>6</sub> -C <sub>9</sub> cycloalkanes	43.8 wt %	28
16	Kraft lignin	280 °C, 6 h, 10.5 MPa	Supercritical ethanol	$\alpha$ -MoC <sub>1-x</sub> /AC	Aromatic monomers	280 mg/g lignin	76
17	Kraft lignin	330 °C, 6 h, 10.5 MPa	Supercritical ethanol	MoC <sub>1-x</sub> /Cu-MgAlO <sub>z</sub>	Aromatic monomers	575 mg/g lignin	77
18	Organosolv lignin	300 °C, 8 h, 7 MPa H <sub>2</sub>	Protic solvents displaying Lewis basicity; Protic solvents displaying no Lewis basicity; Aprotic polar solvents; Aprotic nonpolar solvents	Raney Ni	Abundant products	91 % conversion (in 2-propanol); 81 % conversion (in methylcyclohexane); 86 % conversion (in methanol)	78
19	Corn stover Lignin oligomers	Fractionate 250 °C, 8/10h, 4-5 MPa H <sub>2</sub>	NaOH/H <sub>2</sub> SO <sub>4</sub> Water	Ru, Rh, Pt/Al <sub>2</sub> O <sub>3</sub> , C and NH <sub>4</sub> <sup>+</sup> Z-Y	Lignin oligomers Aromatic hydrocarbons	35 %-60 % conversion	79
20	ATSE-EL; ILOE-EL; ATSE-EHL; ILOE-EHL	235 °C, 2 h, 4 MPa H <sub>2</sub>	Methanol	Pd/C	Bio-oil	61.7 wt %; 57.9 wt %; 34.2 wt %; 45.1 wt %	54
21	Corn stalk/Bamboo /Klason lignin	200-275 °C, 1-3 h, 2 MPa H <sub>2</sub>	Ethanol-water	Ru/C; Pd/C; Pt/C	Bio-oil (4-ethylphenol, 4-ethylguaiacol)	72.9 wt % (3.1 wt %, 1.3 wt %)	80
22	Hydrolyzed lignin	300 °C, 4 h, 2 MPa H <sub>2</sub>	Methanol	Pd/C and CrCl <sub>3</sub>	Aromatic monomers (alkylbenzenes, alkylphenols)	26.3 wt % (6.0 wt %, 12.5 wt %)	81
23	Birch wood	235 °C, 4h, 6 Mpa H <sub>2</sub>	Water; methanol; ethylene glycol	Ni-W <sub>2</sub> C/AC	Phenols (guaiacylpropanol, syringylpropanol, guaiacylpropane, syringylpropane)	36.9 wt % (4.3 wt %, 9.4 wt %, 3.5 wt %, 13.5 wt %); 42.2 wt % (5.3 wt %, 10.6 wt %, 5.8 wt %, 15.8 wt %); 46.5 wt % (5.0 wt %, 9.6 wt %, 5.4 wt %, 18.2 wt %)	82
24	Alkaline lignin	280 °C, 2h, 2 MPa H <sub>2</sub>	Water-ethanol	WP/AC; Ni-WP/AC; Fe-WP/AC	Phenols	67.0 mg/g lignin; 48.8 mg/g lignin; 52.7 mg/g lignin	83
25	Organosolv lignin	130/170 °C, 1/12h, 1 MPa H <sub>2</sub>	Water	Ni <sub>7</sub> Au <sub>3</sub>	Aromatic monomers	14.2 wt %	84
26	Organosolv lignin	130 °C, 1/12h, 1 MPa H <sub>2</sub>	Water	NiRu; NiRh; NiPd	Aromatic monomers	6.8 wt %; 3.6 wt %; 4.6 wt %	85
27	Organosolv lignin	200 °C, 6h, 2 MPa H <sub>2</sub>	Methanol	Ni-Fe/AC	Aromatic monomers	23.2 wt %	86
28	Organosolv lignin; kraft lignin; sugarcane bagasse lignin	225 °C, 2h, 5.8 MPa Ar; 300 °C, 4h, 5 MPa H <sub>2</sub>	Ethanol-water; dodecane	Pt/ $\gamma$ -Al <sub>2</sub> O <sub>3</sub> and NaOH; CoMo/Al <sub>2</sub> O <sub>3</sub> or Mo <sub>2</sub> C/CNF	Lignin-oil; aromatics	9 wt %; 7 wt %; 6 wt %	87

respectively (Table 1, entry 20). The total yield of monomer aromatics in weight of bio-oil was 14.9%, 30.0%, 17.3%, and 14.4% from ATSE-EHL, ATSE-EL, ILOE-EHL, and ILOE-EL, respectively. Ye *et al.*<sup>80</sup> compared the catalysts (Ru/C, Pd/C and Pt/C) effect on the conversion of different lignin (corn stalk lignin/ bamboo lignin/ klason lignin) in ethanol-water solvent in the presence of 2 MPa H<sub>2</sub>. Ru/C exhibited the best effect performance for lignin hydrogenolysis, leading to yield of 3.1 wt % 4-ethylphenol and 1.3 wt % 4-ethylguaiacol from corn stalk lignin at 275 °C (Table 1, entry 21).

Non-noble transition metal (e.g. Ni, Cu) catalysts have been widely used for lignin catalytic hydrogenolysis process. Ni nanoparticles supported on nitrogen-doped carbon (Ni-NDC) prepared via salt-melt synthesis with a hierarchical porosity were estimated to be an efficient catalyst for Kraft lignin hydrogenolysis.<sup>90</sup> The products obtained via hydrogenolysis were different substituted guaiacols. The hydrogenolysis of birch wood lignin for the production of monophenolic compounds was investigated by employing Ni/C catalyst in different alcohol solvents (CH<sub>3</sub>OH, i-PrOH, 1,4-dioxane, glycerol, cyclohexane).<sup>66</sup> In CH<sub>3</sub>OH after 6 h at 200 °C, the highest yield of the monomeric phenols was 54 %, in which 22 % was propylguaiacol and 67 % was propylsyringol (Table 1, entry 4). Raney Ni catalyst was found to be an efficient catalyst for the hydrogenolysis of organosolv lignin in different solvents.<sup>78</sup> After 8h reaction in 2-propanol at 300 °C with 7 MPa H<sub>2</sub>, 91 % lignin was converted to cyclic alcohols, cyclic ketones, and unsaturated products (Table 1, entry 18). Cu-doped porous metal oxide (Cu-PMO) was also effective in lignin hydrogenolysis (Table 1, entry 5-7). The conversion of organosolv lignin to monomeric substituted cyclohexyl derivatives with greatly reduced oxygen content was achieved by using a Cu-PMO catalyst in supercritical methanol (sc-MeOH) at 300 °C.<sup>67</sup> After that, the conversion (about 85 %) of wood and cellulosic samples to bio-oil and bio-gas in a single stage reactor was operated on a Cu-PMO catalyst in sc-MeOH at 300-320 °C.<sup>68</sup> This continuous operation with high yield of C<sub>2</sub>-C<sub>6</sub> aliphatic alcohols (10.0 wt %) and methylated derivatives (5.8 wt %) were suitable for applications as gasoline in principle. Then, catalytic conversion of organosolv lignin to aromatic products was performed on a Cu-PMO catalyst at 180 °C in the presence of H<sub>2</sub>.<sup>69</sup> More than 90 % conversion of lignin with the yield of catechols as 63.7 wt % was obtained after 14h with the optimized catalyst and biomass loading. Cu can favor the desired hydrogenolysis, dehydration, and hydrogenation reactions without hydrogenation the arene rings, leading to obtain catechols from lignin samples. Recently, Sm<sup>3+</sup> has been incorporated into the PMO matrix of the Cu-PMO to give a novel catalyst Cu<sub>20</sub>Sm<sub>5</sub>PMO.<sup>91</sup> Cu<sub>20</sub>Sm<sub>5</sub>PMO catalysts were proved to be more efficient than Cu-PMO for lignin catalytic hydrogenolysis.

Some other novel catalysts have been designed and applied in lignin hydrogenolysis. Ma *et al.*<sup>76</sup> reported the conversion of kraft lignin to chemicals with low molecular weight with an  $\alpha$ -MoC<sub>1-x</sub>/AC catalyst. A maximum yield (280 mg/g lignin) of aromatic compounds was obtained in ethanol (Table 1, entry 16), while no char was observed during this process. Recently, it was reported that the conversion of Kraft lignin over a new designed MoC<sub>1-x</sub>/Cu-MgAlO<sub>2</sub> catalyst can produce some value-added chemicals such as

C<sub>8</sub>-C<sub>10</sub> esters, benzyl alcohols and arenes.<sup>77</sup> MoC<sub>1-x</sub>/Cu-MgAlO<sub>2</sub> catalysts performed much higher activity than the  $\alpha$ -MoC<sub>1-x</sub>/AC catalysts, achieving the highest yield (575 mg/g lignin) of aromatics in ethanol without formation of char or tar at 330 °C (Table 1, entry 17). MoC<sub>1-x</sub>/Cu-MgAlO<sub>2</sub> performed as both homogeneous and heterogeneous simultaneously, producing more radicals and ions from ethanol. This could facilitate the conversion of kraft lignin to small fragments. Transition metal nitrides are biocompatible materials with outstanding physical and chemical properties involving thermal stability and acid resistance. It was reported that transition metal nitrides especially nanoparticulate TiN were promising for the depolymerization of lignin.<sup>70</sup> The prominent aromatic monomer yields (19 wt %) with relatively low char formation can be achieved from lignin hydrogenolysis over TiN in supercritical ethanol at 340 °C (Table 1, entry 8). A new TiN-Ni nanocomposite featured of spherical intergrown core-shell nanoparticles of about 10 nm in diameter was synthesized.<sup>92</sup> Different aryl ethers could be efficiently converted under relatively mild conditions (1.2 MPa, 150 °C) to aromatic compounds and cycloalkanes over TiN-Ni catalyst in few minutes.

### Bimetallic catalyst

The combination of two metals can greatly improve the catalytic performance for the hydrogenolysis of lignin. Zhang *et al.*<sup>84</sup> reported an efficient and stable bimetallic catalyst (NiAu) for lignin hydrogenolysis. 14.2 wt % yield of aromatic monomers were obtained after 12h of reaction under mild reaction conditions (170 °C, 1 MPa H<sub>2</sub>) in pure water (Table 1 entry 25). Au acted as an electron donor in the NiAu catalyst, enabling the conjuncted Ni atoms to be more electronegative. The Ni<sub>7</sub>Au<sub>3</sub> catalyst displayed an outstanding turn-over-frequency (TOF), which was three times more effective than a pure Ni catalyst. A series of bimetallic Ni<sub>85</sub>M<sub>15</sub> (M = Ru, Rh, and Pd) catalysts were further applied in the hydrogenolysis of organosolv lignin with 1 MPa H<sub>2</sub>.<sup>85</sup> The Ni<sub>85</sub>M<sub>15</sub> bimetallic catalyst performed better activity and selectivity compared to that of the single-metal catalysts. The Ni<sub>85</sub>Ru<sub>15</sub> bimetallic catalyst showed the outstanding activity for the lignin hydrogenolysis under low temperature (130 °C) in water, resulting in 6.8 wt % yield of aromatic monomers after 12h of reaction (Table 1 entry 26). The synergistic effect of Ni<sub>85</sub>Ru<sub>15</sub> bimetallic catalyst could be attributed to three reasons: (1) the increment of surface atoms (compared with Ni), (2) the enhancement of hydrogen and substrate activation (compared with Ni), as well as (3) the inhibition of benzene ring saturation (compared with Ru). Recently, the bimetallic catalyst Ni-Fe/AC was proved to be effective for the hydrogenolysis of organosolv lignin.<sup>86</sup> The Ni<sub>1</sub>-Fe<sub>1</sub>/AC (the ratio of Ni/Fe was 1) catalyst gave 23.2 wt % yield of monomer products (mainly propylguaiacol and propylsyringol) at 225 °C with the presence of 2 MPa H<sub>2</sub> (Table 1 entry 27). The Ni-Fe alloy formed in Ni<sub>1</sub>-Fe<sub>1</sub>/AC exhibited outstanding ability for hydrogenolysis of C-O bonds in lignin.

### Bifunctional catalyst

Like the bimetallic catalysts, the bifunctional catalysts (include multifunctional catalysts) could maximize the depolymerization of lignin under the similar conditions compared with that of single

catalysts. The common composition of a bifunctional catalyst is a solid acid catalyst combined with a metal catalyst. Ru/ZrO<sub>2</sub>/SBA-15 and Ru/SO<sub>4</sub><sup>2-</sup>/ZrO<sub>2</sub>/SBA-15 were the effective catalysts to convert pyrolytic lignins to monomer products (phenols, guaiacols, anisoles, esters, light ketones, alcohols and long-chain alkynes) at 260 °C in supercritical ethanol under a hydrogen atmosphere.<sup>93</sup> Bifunctional Ru/Al<sub>2</sub>O<sub>3</sub>, Rh/Al<sub>2</sub>O<sub>3</sub>, Pd/Al<sub>2</sub>O<sub>3</sub> catalysts were used for the catalytic hydrogenolysis of three lignins (alkali lignin, acid lignin and enzymatic lignin) in a formic acid/water reaction system.<sup>71</sup> The main components of phenol, cresol, guaiacol, methylguaiacol, catechol, ethylcatechol, syringol and o-vanillin were found in different concentrations in products from lignin hydrogenolysis with the catalysts. Compared with Rh/Al<sub>2</sub>O<sub>3</sub> and Pd/Al<sub>2</sub>O<sub>3</sub> catalysts, Ru/Al<sub>2</sub>O<sub>3</sub> catalyst achieved the largest amount of highly hydrodeoxygenated monomers (91.5 wt %) after 6h of reaction (Table 1 entry 9). Al<sub>2</sub>O<sub>3</sub> support with Lewis acid sites played a crucial role in the depolymerization of lignin, leading to an increased amount of low molecular weight products. It needs to be noted that these bifunctional catalysts were well established for lignin hydrogenolysis in acid reaction media. Toledano *et al.*<sup>72</sup> described lignin depolymerization to simple aromatics at 140 °C over different metal supported nanoparticles on mesoporous Al-SBA-15 (NiAlSBA-15, PdAlSBA-15, PtAlSBA-15, RuAlSBA-15). 30 wt % of bio-oil was obtained over the NiAlSBA-15 catalyst with formic acid as the hydrogen-donor solvent (Table 1 entry 10). Similarly, the efficient depolymerization of organosolv hydrolyzed lignin in ethanol solvent was achieved using a mesoporous Ni/Al-SBA-15 catalyst.<sup>73</sup> 21.90 wt % monomers yield was obtained, while no char was observed after 4h depolymerization reaction of organosolv hydrolyzed lignin at 300 °C (Table 1 entry 11). In addition, Liguori and Barth<sup>74</sup> reported a Pd catalyst and Nafion® SAC-13 as the solid acid catalyst for catalytic depolymerization of spruce lignin to phenols in water. The yield of phenols (7.7 wt %) was obtained after 21h of reaction at 300 °C (Table 1 entry 12). Guaiacol (2.0 wt %), pyrocatechol (3.7 wt %) and resorcinol (2.0 wt %) were dominated in the phenolic products. As a Brønsted acid, Nafion SAC-13 performed a synergic effect with Pd, promoting the hydrogenolysis reaction over the hydrogenation of aromatic ring.

Bifunctional metal catalysts supported on various zeolites have also been estimated to be highly effective on removing oxygen-containing groups and saturating the aromatic rings.<sup>94</sup> It was reported that the combination of Ru/Al<sub>2</sub>O<sub>3</sub> and HY zeolite was capable for selective conversion of lignin to jet fuel-range hydrocarbons.<sup>55</sup> After 4h of reaction at 250 °C in water, 22 wt % yield of hydrocarbon products could be obtained from the depolymerization of the recovered insoluble lignin (Table 1 entry 13). Recently, Wang *et al.*<sup>75</sup> designed a new catalytic system (Ru-Cu/HY) for converting lignin to biofuels. Ru-Cu/HY was better than the combined catalyst of Ru/Al<sub>2</sub>O<sub>3</sub> and HY zeolite, giving yield of 32 wt % hydrocarbon products at same reaction conditions (Table 1 entry 14). The catalytic ability of Ru-Cu/HY was improved might due to high total and strong acid sites, well dispersion of metal species, as well as high adsorption capacity for -OH groups and C-O bonds. Kong *et al.*<sup>28</sup> reported the conversion of enzymatic corncob lignin to C<sub>6</sub>-C<sub>9</sub> cycloalkanes in dodecane by using Ni supported on amorphous silica-alumina (ASA). This catalyst could directly transform lignin into 43.8 wt% C<sub>6</sub>-C<sub>9</sub>

cycloalkanes with nearly 80 % lignin conversion at 300 °C with 6 MPa H<sub>2</sub> (Table 1 entry 15). The Brønsted acid sites of ASA tailored the electronic distribution of the metal particles, thus enhancing the capability of Ni to cleave ether linkages in lignin.

Multifunctional catalytic matrixes performed excellent selectivity in hydrogenolysis of lignin to aromatic hydrocarbons.<sup>79</sup> A catalytic process was developed for selective depolymerization of lignin polymeric framework and removal of oxygen, including (1) depolymerization of the complex lignin structure to highly reactive low molecular weight intermediates via selective C-O and C-C bond cleavage; (2) substantial reduction of oxygen content in these lignin intermediates to produce phenolic and cyclic hydrocarbons in high yields. Hydrogenolysis of oligomeric technical lignin predominantly containing β-O-4 linkage was performed with supported noble metal catalysts integrated with various solid acid zeolites. It was founded that 35-60 % conversion of lignin together with 65-70 % selectivity of aromatic hydrocarbons (e.g. toluene) was achieved under different hydrogenolysis conditions (250 °C, 8-10h, 4-5 MPa H<sub>2</sub>) in the presence of noble metals (Ru, Rh and Pt) supported on Al<sub>2</sub>O<sub>3</sub> (or C) and NH<sub>4</sub><sup>+</sup> Z-Y 57277-14-1 catalyst matrix (Table 1 entry 19).

An efficient hydrogenolysis process of hydrolyzed lignin was recently performed over a Pd/C catalyst and CrCl<sub>3</sub>.<sup>81</sup> More than 26.3 wt % monomer yield (including 6.0 wt % alkylbenzenes and 12.5 wt % alkylphenols) could be obtained from hydrolyzed lignin at 300 °C, 2 MPa H<sub>2</sub> for 4 h reaction (Table 1 entry 22). Li *et al.*<sup>82</sup> reported the catalytic hydrogenolysis of raw woody biomass to phenols with a carbon supported Ni-W<sub>2</sub>C catalyst in different solvents (water, methanol or ethylene glycol) in the presence H<sub>2</sub>. Different monophenols (guaiacylpropanol, syringylpropanol, guaiacylpropane, syringylpropane) with a highest yield of 46.5 wt % could be obtained at 235 °C after 4h of reaction (Table 1 entry 23). Compared with noble metal catalysts, the cheap catalyst of Ni-W<sub>2</sub>C/AC showed competitive activity for the hydrogenolysis of wood lignin, facilitating the dehydroxylation reaction to give guaiacylpropane and syringylpropane. Tungsten phosphide has been applied as catalyst in cellulose degradation and guaiacol hydrodeoxygenation. The hydrogenolysis of alkaline lignin to phenols with a WP catalyst was reported.<sup>83</sup> The WP/AC catalyst gave the highest yield (67.0 mg/g lignin) of phenols after 2h of reaction in water-ethanol solvent at 280 °C, in which the small weight molecular products mainly composed of 2-methoxy-phenol, 2-methoxy-4-methyl-phenol, 2-methoxy-4-ethyl-phenol, 2-methoxy-4-acetyl-phenol and 2-methoxy-4-propyl-phenol (Table 1 entry 24). It was found that the Ni-WP/AC and Fe-WP/AC catalysts improved the selective production of five phenols but lower the yield of total phenols.

The depolymerization of organosolv, kraft and sugarcane bagasse lignin to produce aromatic products was performed by a two-step method.<sup>87</sup> Firstly, lignin was depolymerized on a Pt/γ-Al<sub>2</sub>O<sub>3</sub> catalyst and NaOH in ethanol-water solvent in the presence Ar. This process lead to a decrease in lignin molecular weight of 32%, 57% and 27% for organosolv, kraft and sugarcane bagasse lignin. Then, the lignin-derived oil was converted to oxygen-free products (highest yield: 24 %) in dodecane under 5 MPa hydrogen over

CoMo/Al<sub>2</sub>O<sub>3</sub> or Mo<sub>2</sub>C/CNF at 300 °C (Table 1 entry 28). Product mixtures from hardwood lignin have a higher oxygen content than that of products obtained from softwood or grass lignin.

Different catalytic processes are involved in lignin hydrogenolysis, such as C-O hydrogenolysis, hydrodeoxygenation, hydrogenation, dehydration, decarboxylation and decarbonylation. The hydrodeoxygenation (HDO) process could increase the energy density of complex biomass molecules, declining their chemical reactivity. Noble metal catalysts do not exhibit better performance than that of non-noble metal catalysts. Compared with monometallic catalysts, the bimetallic catalysts and bifunctional catalysts seem more efficient due to their synergistic effects. The addition of second metal or solid acid catalyst leads to a higher selectivity during hydrogenolysis of lignin, resulting in higher yield of the target products. However, some important drawbacks for heterogeneous catalyst applied in industry should be addressed: 1) the solid catalysts are susceptible to surface saturation and deactivation; 2) the selectivity of solid catalysts for the formation of specific compounds can be further improved, such as inhibiting the hydrogenation of the benzyl ring. Additionally, char formation, condensation reactions and water adsorption cannot be inhibited during lignin hydrogenolysis process.<sup>87</sup> Heterogeneous catalyst for lignin hydrogenolysis needs further development in the following aspects: 1) high selectivity for target products, 2) deep conversion in mild conditions in order to minimize char formation and repolymerization reactions, 3) reusability and hydrothermal tolerance.

### 3.2 Effects of solvent system

Solvent plays an important role in the lignin hydrogenolysis process. Efficient solubilization of lignin will give rise to an efficient lignin hydrogenolysis process.<sup>25</sup> Both electrostatic and polarization interactions are the predominant determinants of the structural properties of dissolution, such as, strong hydrogen bond interactions between ethylene glycol and the free hydroxyl groups present in lignin contribute to the lignin dissolution.<sup>95</sup> Generally, solvents can be divided into four categories: 1) protic solvent displaying Lewis basicity which is considered as both good H-bond donor ( $\alpha$ ), good H-bond acceptor ( $\beta$ ) and Lewis-based solvent; 2) protic solvent displaying no Lewis basicity as the best H-bond donor but not an H-bond acceptor or a Lewis base; 3) aprotic polar solvent which is an H-bond acceptor and a Lewis base; 4) aprotic nonpolar solvent (not an H-bond donor, H-bond acceptor or Lewis acid).<sup>78, 96</sup> Hydrogenolysis of lignin or its model compounds in different solvents will generate different products. Generally, the hydrogenolysis of lignin or its model compounds have been performed in 1) hydrogen-donor solvent system and 2) hydrogen-involved system.<sup>97-99</sup>

#### 3.2.1 Hydrogen-donor solvent system

The lignin hydrogenolysis process has often been associated with significant consumption of hydrogen. In some cases, the use of hydrogen from renewable sources (formic acid, levulinic acid, methanol, ethanol, 2-propanol, etc.) has been performed in lignin hydrogenolysis process.<sup>100</sup> It was proposed that the lignin

hydrogenolysis process is a fragmentation hydrogenolysis process: 1) the depolymerization of lignin to some small fragments; 2) the hydrogenolysis of small fragments to monomers.<sup>66</sup> In both two steps, hydrogen-donor solvent (e.g. ethanol) is essential but plays two different roles, for a solvolysis molecule and for a hydrogen donor, respectively. Hydrogen-donor solvent always plays two roles in the hydrogenolysis process for lignin depolymerization: (1) macromolecule solvolysis and (2) hydrogen-donor.

Different hydrogen-donor solvents in lignin depolymerization reaction could result in a promising change of the ratio and quantities of generated aromatics. The depolymerization of organosolv olive tree pruning lignin in tetraline as hydrogen-donor solvent showed much more amount of guaiacyl derivatives compared to syringyl derivatives; while a 5/1 ratio of syringyl/guaiacyl derivatives was obtained in formic acid as hydrogen-donor solvent.<sup>72</sup> Toledano *et al.*<sup>97</sup> investigated the lignin depolymerization to simple aromatics in various hydrogen-donor solvents (tetralin, isopropanol, glycerol and formic acid). The products were remarkably depended on the type of hydrogen-donor solvent. Highest bio-oil yield with no bio-char was obtained in formic acid, while a maximum of 38 % bio-char was obtained in tetralin. In addition, the hydrogenolysis of native birch wood lignin to monomeric phenols in different alcohol solvents (CH<sub>3</sub>OH, i-PrOH, 1,4-dioxane, glycerol, cyclohexane) was reported.<sup>66</sup> The highest monomer yield (54 %) was obtained in CH<sub>3</sub>OH, where 22 % was propylguaiacol and 67 % was propylsyringol. 27 % yield of monomers was obtained in i-PrOH, where 12 % was propylguaiacol and 37 % was propylsyringol. In 1,4-dioxane, 15 % yield of monomers was obtained, where 6 % was propylsyringol. 16 % yield of monomers was obtained in glycerol, where 16 % was propylguaiacol and 67 % was propylsyringol. The depolymerization of Alcell lignin in different hydrogen-donor solvents (iso-propanol-formic acid; ethanol-formic acid; methanol-formic acid) also resulted in different distribution of aromatic products.<sup>65</sup> Compared to external molecular hydrogen (H<sub>2</sub>), in situ hydrogen-donor resulted in the remarkable yield of oil with the lower O/C ratio and predominant yield in valuable chemical products (e.g. alkylphenolics, aromatics). For iso-propanol, the highest yield of bio-oil was obtained (71 wt%), including 6 wt% alkylphenolics and 11 wt% aromatics. A higher aromatics (17 wt%) and alkylphenolics (7 wt%) yield was obtained in ethanol, while a highest aromatics (19 wt%) and alkylphenolics (11 wt%) yield for methanol, which was the most valuable and desired compounds. It was found that the main ketone products are methyl isobutylketone (MIBK) and mesityloxide (MO), with a 3-4 to 1 ratio of production. These products were likely to be formed from acetone dimerization via an aldol condensation reaction (Fig. 3). And these acetones might be formed by dehydrogenation of iso-propanol and formic acid, which supplied in-situ hydrogen (Fig. 3). Barth *et al.*<sup>101</sup> recently reported that formic acid not only just acts as an in situ hydrogen source or hydrogen donor molecule. Formic acid seemed to react with lignin via a formylation-elimination-hydrogenolysis reaction which gives rise to the depolymerization of lignin. The main effect of the solvent was to stabilize the depolymerized monomers and to form alkoxides, favoring the

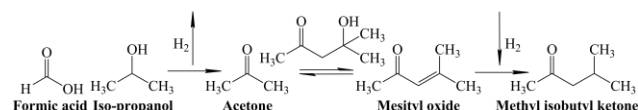


Fig. 3 Reaction schemes for the iso-propanol and formic acid conversion to mesityl oxide and methyl isobutyl ketone reproduced from 65.

elimination/deformylation step. It can be concluded that ethanol is the effective solvent compared with isopropanol and methanol.

Recently, Barrett *et al.*<sup>102</sup> reported that solvent could be applied to control the distribution of products: by adding dimethyl carbonate (DMC), the yield of aromatic products from the Cu<sub>20</sub>PMO-catalyzed hydrogenolysis of lignin model compounds and of organosolv poplar lignin were significantly increased. The MeOH/DMC co-solvent system substantially suppressed arene hydrogenation of the phenolic intermediates, while the unwanted product diversity *via* O-methylation of phenolic -OH groups could produce a lot of stable aryl-OCH<sub>3</sub> species. Thus, reactive alkylphenols undergone selective O-methylation to form alkylmethoxybenzenes and inhibit arene hydrogenation, consequently preserving benzene rings as well as decreasing the unwanted products.

The efficiency (dissolution ability) of solvent is greatly affected by depolymerization reaction condition, especially reaction temperature and pressure.<sup>103</sup> It is reported that the low efficiency of lignin depolymerization process in *i*-PrOH was due to poor dissolution of lignin, while poor hydrogenolysis of lignin in 1,4-dioxane, glycerol and cyclohexane was attributed to the low efficiency of hydrogen-donor under the similar reaction conditions.<sup>78</sup> Under specific conditions, ethanol facilitated the dissolution of lignin, making the reaction mixture a homogeneous phase, which resulted in a high efficiency of lignin depolymerization process.<sup>104</sup> The supercritical hydrogen-donor solvent could achieve unexpected results:<sup>105</sup> no insoluble char was generated by hydrogen-donor from supercritical methanol (sc-MeOH) in the organosolv lignin depolymerization;<sup>67, 106</sup> similarly, no char was formed by hydrogen transfer from supercritical ethanol in lignin depolymerization;<sup>70, 76</sup> the sc-MeOH with great characteristics of dissolution ability and acid-base nature<sup>81</sup> could provide suitable conditions for solubilizing constituent polymers to produce “active lignin”, resulting in higher lignin depolymerization efficiency.<sup>68</sup>

### 3.2.2 Hydrogen-involved system

The lignin hydrogenolysis process based on pressurized molecular hydrogen-involved system has also been widely studied. The hydrogenolysis of organosolv lignin in water in the presence of H<sub>2</sub> has been reported.<sup>85</sup> When > 1.5 MPa H<sub>2</sub>, the product yield was declined because of the high hydrogen coverage over catalyst surface, which prevented the adsorption of substrates. It was also reported that 2.0 MPa H<sub>2</sub> is sufficient for hydrogenolysis of monomeric intermediates.<sup>82</sup> Similar results have been reported that hydrogenation was favored at higher H<sub>2</sub> partial pressure together with methyl group transfer.<sup>107</sup> It can be seen that the hydrogenolysis process with molecular hydrogen as reactant is hard

to control. Thus to improve the controllability of hydrogenolysis process, some hydrogen-donor solvents have been involved in hydrogen-involved system. Parsell *et al.*<sup>108</sup> used CH<sub>2</sub>Cl<sub>2</sub>/methanol as solvent to depolymerize lignin-related polymeric substrates in the presence of H<sub>2</sub>. When the solvent was CH<sub>2</sub>Cl<sub>2</sub>, the aromatic ring was readily hydrogenated to give cyclohexanol, while hydrogenation of aromatic ring was inhibited in methanol.<sup>108</sup> Wang *et al.*<sup>78</sup> reported the hydrogenolysis of lignin in different solvents. 91% conversion of lignin during hydrogenolysis in 2-propanol was achieved. The products were alkanes (particularly, cyclic alkanes), monocyclic alcohols, monocyclic ketones-grouped as saturates and alkenes-grouped as unsaturated compounds. The conversion of lignin in MCH showed 81% conversion while the product selectivity was remarkably turned to the saturated compounds, such as monocyclic and polycyclic alkanes and cyclic alcohols. As for in methanol, the reaction achieved 86% conversion producing mostly phenols. Thus the hydrogen-donor solvent combined with H<sub>2</sub> has significant influence on the distribution of products.

Yield of lignin hydrogenolysis process was not found to be correlated with the H<sub>2</sub> solubility and hydrogen in the system especially high hydrogen pressure does not seem to have positive influence on LDP yields.<sup>96</sup> Recent reports showed that formic acid and alcohols (e.g. methanol, ethanol, isopropanol) as hydrogen source have a lot of advantages than H<sub>2</sub>. Formic acid was reported to be a reactive hydrogen source than external hydrogen atmosphere for hydrogenolysis of lignin. In situ hydrogen from the decomposition of formic acid could participate in the reaction as H atom form, resulting in the higher efficient hydrogen donor than that of external hydrogen.<sup>109</sup> Song *et al.*<sup>66</sup> also reported that molecular H<sub>2</sub> gives no help with lignin conversion, alcohols actually provided active hydrogen species in the reaction. It was considered that the transformation of CH<sub>3</sub>OH to active hydrogen species was easier than that of molecular H<sub>2</sub>, since the bond dissociation energy of the C-H bond (96.1 kcal mol<sup>-1</sup>) of methanol was lower than that of the H-H bond (104.2 kcal mol<sup>-1</sup>) of H<sub>2</sub>. Compared with gaseous hydrogen, hydrogen-donor solvent could suppress repolymerization reaction and char formation in specific situations. Ethanol solvent could inhibit the repolymerization reaction, stabilize the highly reactive phenolic intermediates and preserve the side chain on the aromatic ring.<sup>73, 110</sup> Repolymerization of reaction intermediates could be suppressed by phenol as a hydrogen-donor.<sup>63</sup> Formic acid also could suppress the repolymerization of reaction intermediates.<sup>109</sup> Additionally, demethoxylation reactions could be suppressed and no bio-char was produced with formic acid as a hydrogen-donor.<sup>72</sup>

In lignin hydrogenolysis process, solvent also must be considered in the design of catalytic system. H-bond donor solvent with a larger  $\alpha$  value could activate the substrate through hydrogen bonding, increasing the substrate conversion, while H-bond acceptor solvent with a larger  $\beta$  value should preferentially be adsorbed on the catalyst surface and, hence, suppress the adsorption of substrate on the catalyst.<sup>96, 99</sup> Thus, 1) for aprotic polar solvent, it suppresses the adsorption of substrate on the catalyst, inhibiting the substrate conversion; 2) for aprotic nonpolar solvent, it performs better as solvolysis molecule; 3) for protic solvent, it could activate the substrate, increasing the substrate

conversion. However, H-bond acceptor solvent (aprotic polar solvent and protic solvent displaying Lewis basicity) exhibits unexpected effects in LHP process. Aprotic polar solvent could reduce the catalytic activity towards hydrogenation of aromatic products due to confinement of the adsorption of substrate on the catalyst, improving the selectivity for phenolic products from lignin depolymerization.<sup>78</sup> And protic solvent displaying Lewis basicity could give more amount of reactive chemisorbed hydrogen after dissociative chemisorption over catalyst, improving the substrate conversion. It was reported that the magnitude of the solvent effect on catalytic performance also depended on the metal nature and it was diminished following the order: Ni > Co > Cu.<sup>111</sup> In summary, hydrogen-involved system and hydrogen-donor solvent system can be efficient for lignin depolymerization in presence of the suitable catalysts.

## 4 Hydrogenolysis of lignin-derived model compounds

A great number of research works on catalytic hydrogenolysis of lignin-related model compound are reported in the past decades, in order to give the cracking mechanism of the specific linkages that will be practically hard to get from direct research on lignin. Catalytic reforming of lignin-derived aromatic monomers would be vigorously discussed in this section, together with the catalytic cracking mechanism of typical inter-unit linkages contained in lignin-related aromatic oligomers.

### 4.1 Hydrogenolysis of lignin-derived aromatic monomers

#### 4.1.1 Phenol

The performance of supported Pt, Pd and Ru catalysts for the hydrogenolysis of phenol (*MI*) in water in presence of H<sub>2</sub> was reported.<sup>112</sup> Reaction pathway for *MI* conversion on Pt, Pd and Ru on carbon is shown in Fig. 4. Complete conversion of *MI* to cyclohexanol could be achieved over Pt/C, Pd/C and Ru/C catalysts in water. In the situation of acidic condition (H<sub>3</sub>PO<sub>4</sub>), the highest conversion (94 %) of *MI* to cyclohexane could be achieved over Pt/C. Thus with a Brønsted acid promoter, cyclohexanol could be further dehydroxylated and hydrogenated to the alkane product. Besides activating ether bonds, Brønsted acidity improves the hydrogenation performance of the Pt/C catalyst. It is in accordance with the report that the Brønsted acid sites in the vicinity of metal could result in the promotion in reaction rate of hydrogenolysis.<sup>113</sup> Similarly, Ni/HZSM-5 and Ni/Al<sub>2</sub>O<sub>3</sub>-HZSM-5 catalysts were used for the hydrogenolysis of *MI* in water with presence of H<sub>2</sub>.<sup>114</sup> It was found that the cyclohexanol dehydration reaction rate mainly depended on Brønsted acid site concentration of catalyst. The Al<sub>2</sub>O<sub>3</sub> binder with Lewis acidity stabilized a ketone intermediate and inhibited the hydrogenation reaction. The reaction rate was increased as the sequence: phenol hydrogenation < cyclohexanone hydrogenation < cyclohexanol dehydration << cyclohexene hydrogenation. The phenol hydrogenation reaction was rate-controlling step. The Ni/Al<sub>2</sub>O<sub>3</sub>-HZSM-5 catalyst showed a catalytic activity for *MI* hydrogenation about five times higher than that of Ni/HZSM-5 due to the evenly Ni dispersion. Reaction pathway for

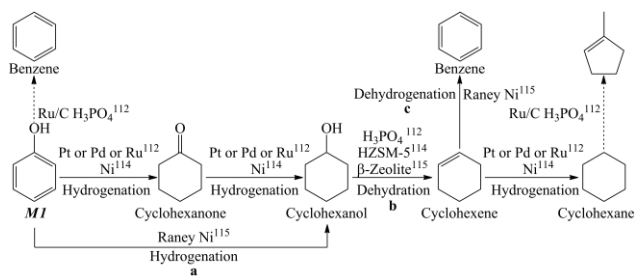


Fig. 4 Reaction mechanism for phenol (*MI*) conversion over the catalysts.

*MI* conversion on Ni/HZSM-5 and Ni/Al<sub>2</sub>O<sub>3</sub>-HZSM-5 is shown in Fig. 4.

Wang *et al.*<sup>115</sup> proposed a novel pathway for the conversion of *MI* into arenes. The one-pot process was conducted at 160 °C over Raney Ni and  $\beta$ -zeolite catalysts with 2-propanol (2-PrOH) as hydrogen-donor solvent in a molar ratio of 2-PrOH/phenol between 1-3. 82 % yield of benzene was achieved with molar ratio of 2-PrOH/phenol = 1.5, and the weight ratio of solid acid/Raney Ni = 0.133. The pathway for phenol dehydroxylation consisted of the hydrogenation of *MI* to cyclohexanol (a), dehydration of cyclohexanol to cyclohexene (b) as well as dehydrogenation of cyclohexene to benzene (c) (Fig. 4). In presence of pressurized H<sub>2</sub>, it was impossible to conduct step (a) and step (c) in the one-pot process. But this one-pot process was initiated by H transfer without using molecular H<sub>2</sub>, step (a) and step (c) became compatible in the process.

#### 4.1.2 4-propylphenol

Hydrogenolysis of 4-propylphenol (*M2*) over a series of activated carbon (AC) doped with Pt, Pd, Rh and Ru catalysts in water in presence of H<sub>2</sub> was reported.<sup>116</sup> The Pt/AC(N) catalyst showed significant high catalytic ability, giving propylcyclohexane in 97% yield. Reaction pathway for *M2* conversion over catalysts is shown in Fig. 5. Rh, Ru, and Pd catalysts supported on AC(N) gave lower yield of propylcyclohexane than that of Pt/AC(N) catalyst. Bimetallic Pt-M/ZrO<sub>2</sub> (M=Re, Sn, Ir, Ga, Fe, Au, Pd, W, In, Mo, Bi) catalysts were also developed for the selective hydrogenolysis of *M2* to n-propylbenzene in presence of H<sub>2</sub>.<sup>117</sup> Pt-Re/ZrO<sub>2</sub> was found to be the most effective catalyst, giving n-propylbenzene yield of 57% with 85% selectivity. The catalyst deactivation was mainly attributed to the water-induced wrapping of Pt nanoparticles by ZrO<sub>2</sub> like the SMSI phenomenon. The addition of Re to Pt/ZrO<sub>2</sub> improved the catalyst stability (prevent the Pt sintering) and product selectivity. Reaction pathway for *M2* conversion on Pt-Re/ZrO<sub>2</sub> catalyst is shown in Fig. 5. Unlike the reaction pathways of *M2* over Pt/AC(N) catalyst, the pathways (a) hydrogenation of *M2* to propylcyclohexanol, (b) dehydration of propylcyclohexanol to propylcyclohexene and (c) dehydrogenation of propylcyclohexene to propylbenzene were involved with high efficiency even at 280 °C.

#### 4.1.3 Guaiacol

The hydrodeoxygenation of guaiacol (*M3*) has been conducted in a batch reactor over Al<sub>2</sub>O<sub>3</sub>- and SBA-15 SiO<sub>2</sub>-supported

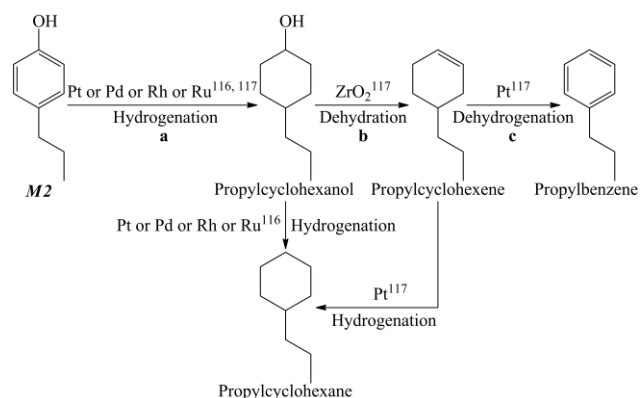


Fig. 5 Reaction mechanism for 4-propylphenol (**M2**) conversion over the catalysts.

molybdenum nitride catalysts at 300 °C in the presence of 5 MPa H<sub>2</sub>.<sup>118</sup> The SiO<sub>2</sub>-supported catalysts gave minimum catechol production and maximum phenol production, while the Al<sub>2</sub>O<sub>3</sub>-supported catalysts produced more catechol than phenol. It was suggested that Al<sub>2</sub>O<sub>3</sub>-supported catalysts proceeded via both the demethylation (DME) and demethoxylation (DMO) routes, while the SiO<sub>2</sub>-supported catalysts proceeded primarily via DMO route. The prefer for DME and methylation pathways of the Al<sub>2</sub>O<sub>3</sub>-supported catalysts was affected by its higher total acidity. Reaction pathways for **M3** conversion over MoN/Al<sub>2</sub>O<sub>3</sub> and MoN/SBA-15 catalysts are shown in Fig. 6. The conversion of **M3** over a Pt/γ-Al<sub>2</sub>O<sub>3</sub> catalyst at 300 °C under 140 kPa H<sub>2</sub> in a flow reactor was also reported.<sup>107</sup> A number of products were obtained, where the significant products were designated to phenol, catechol and 3-methylcatechol. Three types of reactions have been addressed during the process: DME (a), hydrodeoxygenation (HDO) (b), and transalkylation (c) (Fig. 6). In addition, the hydrodeoxygenation of **M3** over a commercial sulfided CoMo/Al<sub>2</sub>O<sub>3</sub> catalyst was performed in dodecane at 300 °C in presence of 5 MPa hydrogen.<sup>119</sup> It was also found that the DME pathway was favorable over the direct DMO pathway on the sulfided CoMo/Al<sub>2</sub>O<sub>3</sub> catalyst. Similarly, the hydrodeoxygenation of **M3** on the classical sulfided CoMo and NiMo/Al<sub>2</sub>O<sub>3</sub> catalysts in tetradecane exhibited that reaction pathway for **M3** conversion was initiated with DME and HDO, followed by benzene ring saturation (Fig. 6).<sup>120</sup> Hydrodeoxygenation of **M3** over carbon nanofiber-supported (CNF) W<sub>2</sub>C and Mo<sub>2</sub>C catalysts was performed in dodecane at 300–375 °C under 5.5 MPa H<sub>2</sub>.<sup>121</sup> Selectivity of up to 87 % and 69 % for phenol and methylated phenolics were obtained with the conversion over 99% at 375 °C over W<sub>2</sub>C/CNF and Mo<sub>2</sub>C/CNF, respectively. The Mo<sub>2</sub>C/CNF catalyst exhibited a better performance than W<sub>2</sub>C/CNF, producing substantial deoxygenated aromatics such as benzene and toluene. The conversion of **M3** to phenol over W<sub>2</sub>C/CNF and Mo<sub>2</sub>C/CNF catalysts did not undergo DME and sequential HDO pathway, but a direct DMO route (Fig. 6). It can be determined that the acidic supports on the catalyst could result in the high preference for demethylation and transalkylation.

Hydrogenation (25 %) and hydrogenolysis through demethoxylation of the C<sub>aryl</sub>-OMe bond (75 %) of **M3** proceeded in parallel over a Ni/HZSM-5 catalyst, resulting in 2-

methoxycyclohexanol and phenol as main products (Fig. 7).<sup>113</sup> The remained hydrogenated 2-methoxycyclohexanol was converted either via cleavage of the C<sub>alkyl</sub>-OMe bond on Ni forming methanol and cyclohexanol, or through acid mediated routes toward the formation of cyclohexanol and cyclopentylmethanol. Güvenatam *et al.*<sup>112</sup> reported a similar reaction pathway for the hydrodeoxygenation of **M3** on Pt/C, Pd/C and Ru/C catalysts in water in presence of H<sub>2</sub> (Fig. 7). Pt/C and Ru/C were trended to promote demethoxylation of **M3** to phenol, initiating a route toward selective formation of cyclohexanol (Route A in Fig. 7). However, Pd/C could promote the direct hydrogenation of the arene ring prior to deoxygenation, leading to 2-methoxycyclohexane as an intermediate product that can be further isomerized and hydrogenated to methyl-1,2-cyclohexanediol (Route B in Fig. 7). Recently, Kim *et al.*<sup>122</sup> also reported the hydrodeoxygenation of **M3** with 2-propanol as a hydrogen donor and RuRe/C catalysts. In accordance with Güvenatam's report, demethoxylation of **M3** to phenol can be significantly promoted by RuRe/C, followed by hydrogenation to cyclohexanol as Route A in Fig. 7, whereas Route B was not favorable. The addition of Re to Ru/C catalysts could enhance the reaction of C-O hydrogenolysis, and promote the production of cyclohexane.

Some studies have proposed that the hydrodeoxygenation of guaiacol in specific system followed only one route. The hydrodeoxygenation of **M3** on mono- and bimetallic Rh-based catalysts in tetradecane at 400 °C under 5 MPa hydrogen was reported.<sup>120</sup> The Rh-based catalysts showed the best performance, but lead to hydrogenation the aromatic rings. Reaction pathway for **M3** conversion by Rh-based catalysts involved saturation of the guaiacol aromatic ring, and subsequently demethoxylation and dehydroxylation of oxygenates (Route B in Fig. 7). In addition, the hydrodeoxygenation of **M3** was performed over the bifunctional Rh/SiO<sub>2</sub>-Al<sub>2</sub>O<sub>3</sub> and Ru/SiO<sub>2</sub>-Al<sub>2</sub>O<sub>3</sub> catalysts in n-decane at 250 °C under 4 MPa hydrogen.<sup>123</sup> The reaction pathway on Rh/SiO<sub>2</sub>-Al<sub>2</sub>O<sub>3</sub> and Ru/SiO<sub>2</sub>-Al<sub>2</sub>O<sub>3</sub> catalysts also followed the Route B. The hydrodeoxygenation of syringol over Ni/SiO<sub>2</sub>-Al<sub>2</sub>O<sub>3</sub> catalyst under a mild condition (200 °C and 2 MPa H<sub>2</sub>) followed the Route A in Fig. 7: occurred the demethoxylation of syringol to form guaiacol, followed by demethoxylation and dehydroxylation to form benzene, hydrogenated to cyclohexane eventually.<sup>124</sup>

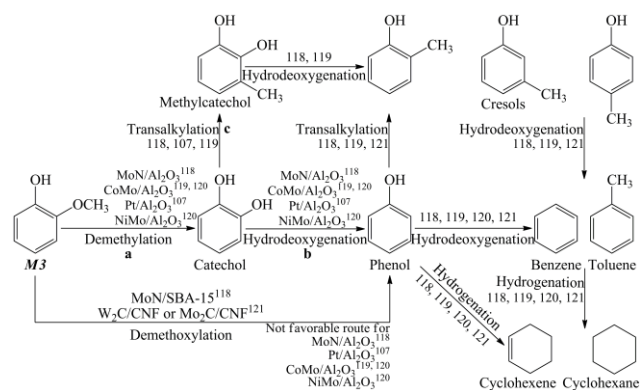


Fig. 6 Reaction mechanism (1) for guaiacol (**M3**) conversion over the catalysts.

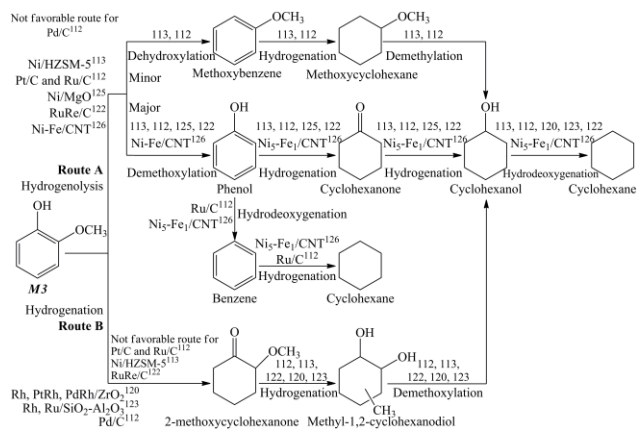
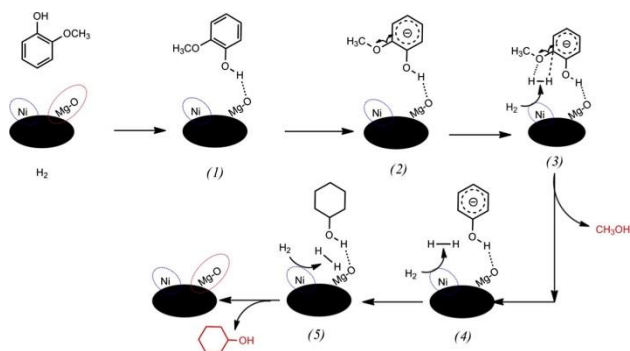


Fig. 7 Reaction mechanism (2) for guaiacol (**M3**) conversion over the catalysts.

Under 160 °C and 3 MPa  $H_2$ , 97.7 % of **M3** conversion with 100 % cyclohexanol selectivity could be attained over a 20 % Ni/MgO catalyst.<sup>125</sup> The reaction pathway on Ni/MgO catalysts followed Route A in Fig. 7. It was proposed that the efficient promotion of the base-carrier for Ni active center was responsible for **M3** conversion as well as dehydroxylation inhibition. The catalytic mechanism for **M3** hydrogenation over the Ni/MgO catalyst was shown in Scheme 1. The acid-base effect between the phenolic hydroxyl group and MgO could lead to the high conversion and selectivity. Fang *et al.*<sup>126</sup> reported the catalytic hydrodeoxygenation of **M3** on Ni-Fe/CNT catalysts at 300 °C under 3 MPa hydrogen. Reaction pathway for **M3** conversion was changed by tuning the Ni/Fe atomic ratios. Like the reaction pathway of **M3** on Ni/MgO catalysts, 99.8% selectivity to cyclohexane could be obtained over Ni-Fe/CNT catalysts with Ni/Fe atomic ratios of 5/1, while 83.7% selectivity to phenol could be obtained over Ni-Fe/CNT catalysts with Ni/Fe atomic ratios of 1/5 (Route A in Fig. 7). This selectivity-switchable performance was attributed to the synergism among Ni domains, where molecule  $H_2$  can be easily activated and the strong oxophilicity was exhibited on the Fe domains.

Compared reaction pathway (1) with reaction pathway (2) (Fig. 6 and Fig. 7), it could be concluded that noble metals are responsible for the hydrogenation of aromatic rings while metal-doped acidic supports are indispensable to the deoxygenation of oxygenates. Classical sulfided CoMo and NiMo catalysts exhibited potential in producing aromatics, but were relatively inert and produced significant coke compared to noble metals.



Scheme 1. Catalytic mechanism for guaiacol hydrogenation over the Ni/MgO catalyst, adapted from 125.

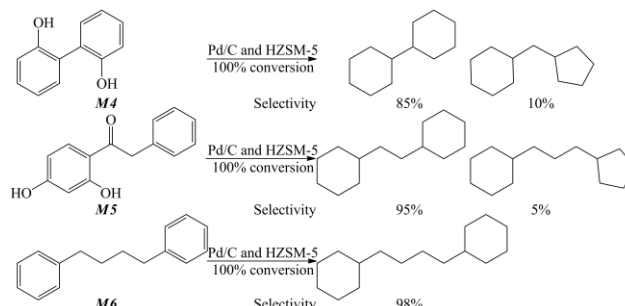


Fig. 8 Hydrodeoxygenation of phenolic dimers on Pd/C and HZSM-5 catalysts in water, reproduced from 127.

## 4.2 Reductive cleavage of typical inter-unit linkages in lignin-derived oligomers

### 4.2.1 C-C linkage

Some of the carbon-carbon bonds in lignin is difficult to be cleaved, such as  $\beta$ -1,  $\beta$ - $\beta$  bonds. The development of catalysts for the linkage cracking (particularly the aryl-aryl linkages) is considerably challenging. The hydrodeoxygenation of a variety of C-C bond contained model compounds such as 5-5' (**M4**),  $\beta$ -1 (**M5**) and  $\beta$ - $\beta$  (**M6**) was performed over Pd/C and HZSM-5 catalyst in water at 473 K and 5 MPa  $H_2$ .<sup>127</sup> It was found that the C-C linkages in 5-5',  $\beta$ -1, and  $\beta$ - $\beta$  were maintained, whereas the substituted hydroxyl and ketone groups were selectively removed, resulting in > 95% yields of hydrodeoxygenated  $C_{12}$ ,  $C_{14}$ , and  $C_{16}$  bicycloalkanes, respectively (Fig. 8). The hydrodeoxygenation of  $\beta$ -1 dimer diphenylmethane (DPM) and 5-5' dimer biphenyl model compounds was performed on Pt/C, Pd/C and Ru/C catalysts in water in presence of  $H_2$ .<sup>112</sup> With the same pathway over Pd/C and HZSM-5 catalyst, the reaction only result in rapid saturating the aromatic rings completely. It might be due to the fact that the intramolecular hydrogen bonds in these model compounds not only promote the stability of the aromatic ring, but also affect the spatial configuration of two benzene rings hindering the access of the catalyst.<sup>127</sup>

### 4.2.2 C-O linkage

A number of different ether linkages exist in lignin, where the most abundant linkage is the  $\beta$ -O-4 linkage. The ether linkages, such as  $\alpha$ -O-4, 4-O-5 and  $\beta$ -O-4, can be readily cleaved, while the general reaction pathways are depicted below.

The hydrodeoxygenation of a variety of C-O bond contained model compounds such as  $\alpha$ -O-4, 4-O-5 and  $\beta$ -O-4 was performed over Pd/C and HZSM-5 catalyst in water at 473 K and 5 MPa  $H_2$ .<sup>127</sup> The benzylphenyl ether (**M7**) and the *o*- or *p*-hydroxyl-substituted  $\alpha$ -O-4 model compounds (**M8**, **M9**) were converted with 50 % yield of  $C_6$  cyclohexane and 50% yield of  $C_7$  methylcyclohexane (Fig. 9). The 4-O-5 dimer diphenyl ether (**M10**) and 4-hydroxy-substituted diphenyl ether (**M11**) were converted to  $C_6$  cyclohexane (Fig. 10). The  $\beta$ -O-4 model compound (**M12**) was also converted to 46%  $C_6$  cyclohexane and 54%  $C_8$  ethylcyclohexane (Fig. 11). The combined of Pd/C with HZSM-5 exhibited an extremely good performance in removing oxygen-containing groups in lignin-related model dimers. In the presence of phosphoric acid and  $H_2$ ,

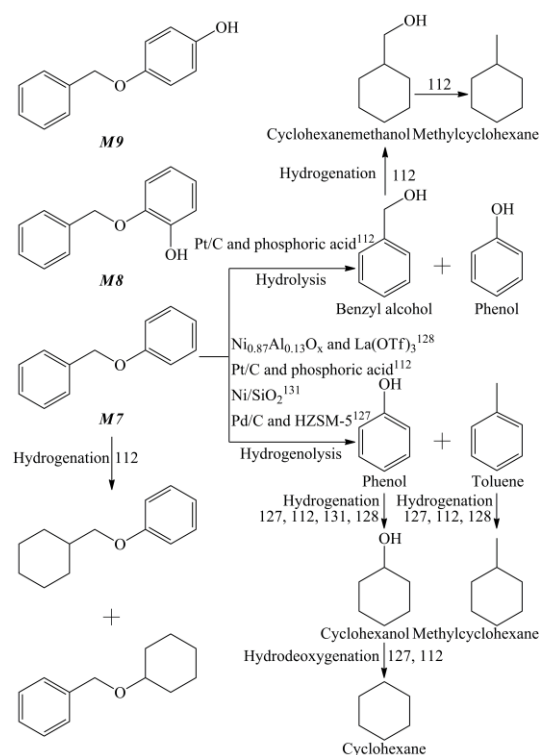


Fig. 9 Reaction pathways for  $\alpha$ -O-4 bond contained model compounds conversion on the catalysts.

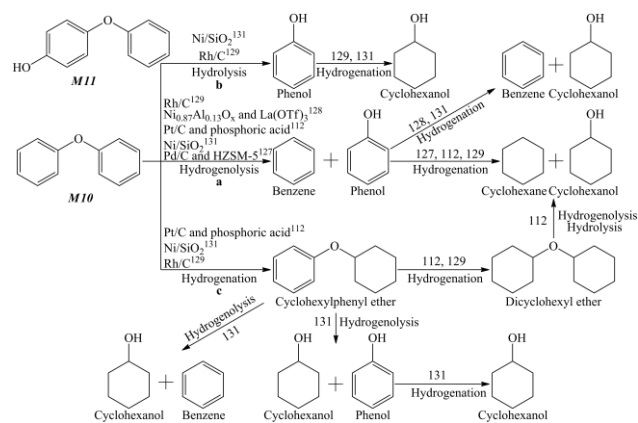


Fig. 10 Reaction pathways for 4-O-5 bond contained model compounds conversion on the catalysts.

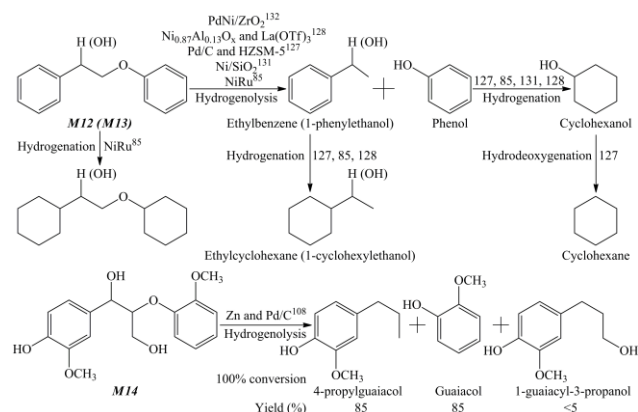
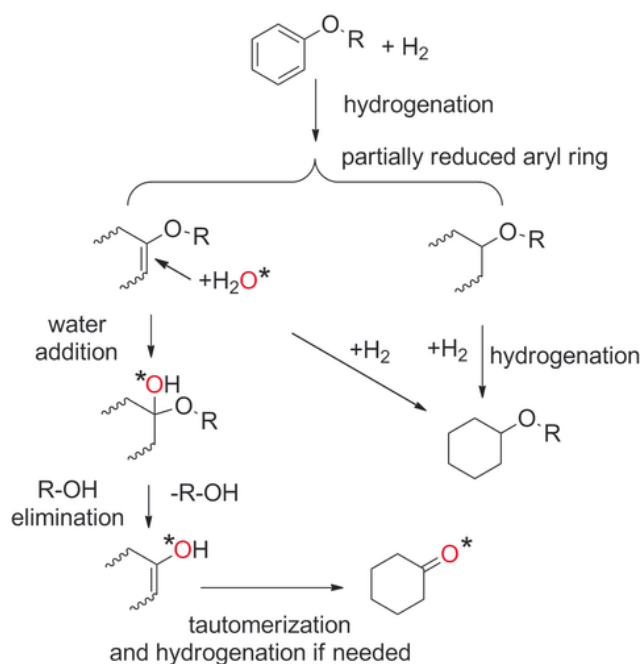


Fig. 11 Reaction pathways for  $\beta$ -O-4 bond contained model compounds conversion on the catalysts.

the conversion of **M7** and **M10** was performed on a Pt/C catalyst in water.<sup>112</sup> The **M7** conversion was 95% after 0.5 h, predominantly yielding methylcyclohexane (42%), cyclohexane (23%) and phenol (15%). Cleavage of the C-O linkage could occur via either the acid-catalyzed hydrolysis or Pt-catalyzed hydrogenolysis pathway (Fig. 9). For **M10**, nearly quantitative **M10** was converted to cyclohexane. The direct hydrogenolysis toward cyclohexanone and cyclohexane was in competition with direct hydrogenation of the aromatic rings toward dicyclohexyl ether. It would be followed by either an acid-catalyzed hydrolysis or Pt-catalyzed hydrogenolysis reaction leading to the formation of cyclohexanol and cyclohexane (Fig. 10). In the presence of a Lewis acid and H<sub>2</sub>, the hydrogenolysis of **M7**, **M10** and **M12** on a NiAlO<sub>x</sub> catalyst in isopropanol was demonstrated.<sup>128</sup> Combination of Ni<sub>0.87</sub>Al<sub>0.13</sub>O<sub>x</sub> and La(OTf)<sub>3</sub> exhibited the highest activity. Full conversion was achieved in the case of **M7** and cyclohexanol was observed with 99% yield at 120 °C after 2h. Reaction pathway of **M7** conversion was shown in Fig. 9. Hydrogenolytic cleavage of **M10** produced benzene and cyclohexanol (93%) in good yields (Fig. 10). In the case of **M12**, full conversion and high selectivity (99%) to cyclohexanol were achieved (Fig. 11). In this catalytic system, the activation of the corresponding C-O bond by La(OTf)<sub>3</sub> was constituted of a crucial step in the catalytic cycle, while arene hydrogenation was suppressed in this step in the presence of La(OTf)<sub>3</sub>. The hydrogenolysis of **M10** was performed over a Rh/C catalyst in supercritical carbon dioxide (scCO<sub>2</sub>)/water under mild reaction conditions.<sup>129</sup> The conversion of **M10** lead to the formation of cyclohexanol with a high selectivity of 96% in water at 80 °C, 0.5 MPa H<sub>2</sub> and 10 MPa CO<sub>2</sub>. The conversion of **M10** followed (a) hydrogenolysis/hydrogenation, (b) hydrolysis/hydrogenation and (c) hydrogenation (Fig. 10). Hydrogenolysis and/or hydrolysis dominated over hydrogenation at low H<sub>2</sub> pressure. In addition, the cleavage of **M13** was performed on NiRu catalysts in water under low temperature (100 °C) and low H<sub>2</sub> pressure (0.1 MPa).<sup>85</sup> The Ni<sub>85</sub>Ru<sub>15</sub> catalyst showed high activity in **M13** hydrogenolysis, achieving 100 % conversion and 95.7 % monomers yield. Reaction pathway of **M13** conversion was shown in Fig. 11. Recently, a novel pathway for the Pd-catalyzed reductive hydrolysis of aryl ethers was proposed.<sup>130</sup> This pathway is distinct from either metal-mediated direct ether cleavage or acid-catalyzed ether cleavage pathway (above pathways). Aryl ethers was initiated by partial hydrogenation of the arene ring to enol ether intermediates, followed by water attack to form a hemiacetal rapidly, converted to cyclohexanone and phenol/alkanol products (Scheme 2).

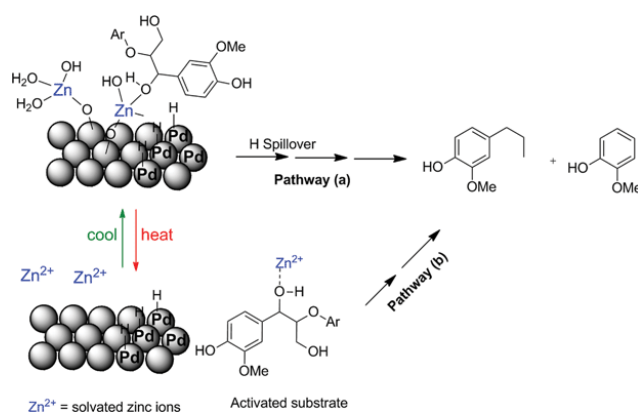
The C-O bond contained model compounds can be selectively deoxygenated without hydrogenation of the aromatic ring. Selective cleavage of **M7**, **M10** and **M12** over a Ni/SiO<sub>2</sub> catalyst at 120 °C in presence of 0.6 MPa H<sub>2</sub> was reported.<sup>131</sup> The reaction pathway for **M7** conversion was dominated by the hydrogenolysis of **M7** to toluene and phenol, followed by a small extent of hydrogenation of phenol to cyclohexanone and cyclohexanol (Fig. 9). Hydrogenolysis was the dominant reaction for the cleavage of **M12**, resulting in ethylbenzene and phenol as the primary products (Fig. 11). The two major routes for **M10** conversion (Fig. 10) was proposed: (a) hydrogenolysis of **M10** to benzene and phenol, and then phenol is rapidly hydrogenated to cyclohexanol, and (b) hydrolysis of **M10** to two molecules of phenol, followed by



Scheme 2. Speculated reaction pathways for the reductive hydrolysis of aryl ethers on Pd surfaces. R=phenyl, cyclohexyl, phenylethyl, and *n*-butyl, adapted from 130.

hydrogenation to cyclohexanol; minor route (c): hydrogenation of **M10** to cyclohexylphenyl ether, and sequentially to be hydrolyzed or hydrogenolyzed to cyclohexanol, benzene, and phenol. Phenol is hydrogenated to cyclohexanol, and a small amount of benzene is hydrogenated to cyclohexane. Similarly, the hydrogenolysis of **M7**, **M10** and **M12** was successfully performed on TiN-Ni catalyst in ethanol at 1.2 MPa.<sup>92</sup> Full conversion of **M7** was achieved at 125 °C, phenol and toluene were the sole products. Full conversion of **M12** was achieved at 150 °C while cyclohexanol and ethylbenzene were the sole reaction products. Full conversion of **M10** was achieved at 150 °C, while cyclohexanol and benzene were the main products. And the Cu<sub>20</sub>Sm<sub>5</sub>PMO catalyst showed its potential in the hydrogenolysis of **M7**, **M10** and **M12**.<sup>91</sup> It can be found that phenol derivative is the major product from the hydrogenolysis process, in spite of the model compounds.

Due to the “synergistic effects”, bimetallic catalysts with superior activity over the corresponding mono-metallic catalyst as well as lower hydrogenation selectivity have been widely applied in the hydrogenolysis of lignin model compounds. A bimetallic Pd/C and Zn catalytic system was described<sup>108</sup> which can effectively cleave **M14** with conversions between 80-90 % in methanol at 150 °C under 2 MPa H<sub>2</sub> (Fig. 11). The proposed mechanisms for the synergy between Zn<sup>2+</sup> and Pd was showed in Scheme 3. Pathway (a) involved substrate binding to Zn<sup>2+</sup> sites and hydrogen spillover from Pd sites. Pathway (b) represented desorption of Zn ions into solution, activating substrate through binding, and Zn-bounding substrate that reacts with Pd sites on the surface of catalyst. Highly dispersed Pd-Ni bimetallic nanoparticles immobilized on ZrO<sub>2</sub> was proved to be an effective catalyst for the hydrogenolysis of **M13** under H<sub>2</sub> at atmospheric pressure.<sup>132</sup> The cleavage of **M13** leads to the formation of phenol with high selectivity of 97% in ethanol at 80 °C with the addition of NaBH<sub>4</sub> (Fig. 11). The hydrogenation of



Scheme 3. Proposed mechanisms for hydrogenolysis of  $\beta$ -O-4 bond contained lignin substrate over Zn and Pd/C catalyst, adapted from 108.

phenol reaction could be controlled by the amount of NaBH<sub>4</sub>, while the nickel depressed the hydrogenation to a certain extent. A Ni<sub>1</sub>-Fe<sub>1</sub>/AC (the ratio of Ni and Fe was 1:1) catalyst exhibited good performance in C-O bond cleavage of **M14** without hydrogenation of arene ring.<sup>86</sup> **M14** could be depolymerized by Ni<sub>1</sub>-Fe<sub>1</sub>/AC to 100% of guaiacol, 88% of propylsyringol and 12% 4-(3-hydroxypropyl)-2,6-dimethoxyphenol at 200 °C under 2 MPa H<sub>2</sub>. The aromatic rings was retained in **M14** depolymerization reaction, since Fe inhibited hydrogenation activity from nickel through the geometric effects.<sup>126</sup> Recently, Zhu *et al.*<sup>18, 133</sup> investigated the selective cleavage of  $\beta$ -O-4 bonds in lignin model compounds over Pd/C and formate as catalysts under microwave irradiation, together with the influence of the benzylic alcohol, aromatic methoxyl and phenolic hydroxyl groups on the cleavage of  $\beta$ -O-4 bonds in lignin model compounds. The benzylic alcohol group resulted in a complicated product distribution and hindered the cleavage of  $\beta$ -O-4 bonds. The aromatic methoxyl group in both non-phenolic and phenolic compounds promoted the cleavage of  $\beta$ -O-4 bonds with the reactivity in order of syringyl (S) > guaiacyl (G) > *p*-hydroxyphenyl (H) units. The phenolic hydroxyl group had a mildly negative impact on the cleavage of  $\beta$ -O-4 bonds.

In summary, most of the model compounds are found to be converted to phenols or substituted phenols, and acetophenone or propyl-aromatics from (catalytic) hydrogenolysis process. The hydrogenolysis of lignin model compounds over noble metal catalysts such as Pt, Ru, Rh and Pd catalysts may fully saturate arene rings, producing cyclic alcohols and cycloalkanes. However, the hydrogenolysis of lignin model compounds over non-noble metals such as Ni, Cu catalysts could introduce selective cleavage of C-O bonds in lignin model compounds without attacking the arene rings.

## 5 Novel technologies for lignin depolymerization in solvent

### 5.1 Two-step LDP (lignin depolymerization)

Two-step LDP (lignin depolymerization) including 1) selective oxidation of benzylic alcohols without C-O or C-C cleavage or  $\gamma$ -alcohol dehydrogenation<sup>134, 135</sup>, 2) reductive cleavage of C-O or C-

C bonds, are attracting more and more attentions because of the high yield of aromatic monomers. Rahimi *et al.*<sup>136</sup> reported the conversion of an oxidized lignin to produce a number of aromatic monomers. Original lignin can be converted to the structurally identified monomeric aromatics with the yield of 52%.<sup>137</sup> The initial selective oxidation of a C<sub>α</sub>-OH to a ketone activated the cleavage of C-C or C-O linkage in the second step.<sup>138</sup> A redox-neutral reaction was mediated by formate and formic acid, giving rise to no consumption of formic acid in whole process (Fig. 12). The C<sub>α</sub> ketone was vital in this two-step LDP, which lowered the barrier for the rate-controlled step of E2 elimination. This rate-controlled elimination step involved both a base (formate) to remove the proton and an acid (formic acid) to assist the loss of the formate.

Lancefield *et al.*<sup>139</sup> also has performed the chemoselective oxidation of β-O-4 linkage in lignin model compounds as well as lignin in the DDQ/*t*BuONO/O<sub>2</sub>. The oxidized β-O-4 linkage can be cleaved in the following reaction over Zn. This approach could be performed in one pot, resulting in a simple mixture of products with high selectivity. The depolymerization of birch lignin obtained the phenolic monomer as the major product with the yield of 5 wt %. Two advantages of the approach can be summarized as: (1) high selectivity for specific aromatic compounds; (2) preservation of functional groups in dominating phenolic monomers.

Jiang *et al.*<sup>140</sup> developed a new approach (via a two-step process) to catalytic convert corncob residue lignin to mono-phenols, inhibiting remarkable degradation of the cellulose component. This approach could achieve high yield and selectivity of mono-phenols, and the remained residue with high content of cellulose (83.5 %) was a promising feedstock for producing biofuel. Firstly, the lignin component in corncob residue was selectively converted to oligomers in the H<sub>2</sub>O-THF (3:7, v/v), where the conversion of lignin reached up to 89.8 % at 200 °C for 1.0 h. Then, a further conversion of oligomers to mono-phenols, giving 24.3 wt % yield of mono-phenols at 300 °C without the presence of H<sub>2</sub>. 4-Ethylphenol (10.5 wt %), 2,6-dimethoxyphenol (6.6 wt %), and 4-ethylguaiaicol (4.0 wt %) counted about 86.8 % of obtained monomers.

## 5.2 Methods to avoid repolymerization of the produced fragments

Because of the evolution of radicals during lignin depolymerization in harsh condition and/or self-condensation reactions, a complex pool of the re-condensed aromatic fragments can be triggered for the formation of undegradable molecules and char.<sup>141-143</sup> To suppress repolymerization reactions in base-catalyzed system for lignin depolymerization, boric acid and phenol were studied as the capping agents.<sup>144</sup> Boric acid and phenol were found to play different role: in phenol-involved experiments high quantities of monomeric phenolic compounds (cresols, catechols, ferulic acid) were yielded; but in boric acid-involved experiments, repolymerization was slightly prevented resulting in the large production of char. It can be suggested that boric acid trapped reaction intermediates and restricted product formation,

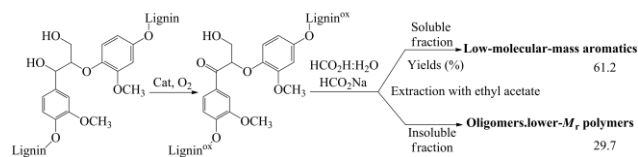


Fig. 12 Depolymerization of oxidized aspen lignin in formic acid/formate, reproduced from 136.

producing oligomers, while phenol prevented repolymerization without inhibiting the demethoxylation and dealkylation reactions.

Deuss *et al.*<sup>145</sup> presented a novel approach in catalytic depolymerization of lignin. The key innovation was in situ conversion of reactive intermediates, formed during lignin depolymerization, to aromatic monomers. Reactive fragments (aldehyde products) were captured in situ by a catalytic reaction with ethylene glycol or by hydrogenation or by decarbonylation, obtaining high yields of three types of aromatic monomers (acetals, ethanol and ethyl aromatics, and methyl aromatics). Acetal formation with ethylene glycol, metal-catalyzed hydrogenation to provide aromatics and catalytic decarbonylation to give methyl aromatics confirmed the approach for aldehyde stabilization. The reactivity of a broad range of metal triflates in catalytic reactions with ethylene glycol was evaluated together with catalytic decarbonylation of different lignin-related model compounds.<sup>146</sup> Product distribution from the model compound depolymerization was significantly related to the type of metal triflate used. As for lignin, Fe(OTf)<sub>3</sub> was proved to be very active and the phenolic C2-acetal products were obtained in a high yield as 19.3 ± 3.2 wt%. Recently, a class of (β-O-4)-(β-5) contained lignin model compounds were synthesized to represent the abundant lignin fragment (particularly in softwoods), in order to gain insight into the acid-catalyzed cleavage of the linkages in lignin by using ethylene glycol.<sup>147</sup> Ethylene glycol played an effective role in trapping the formaldehyde released not only from the β-O-4 linkage but also the β-5 linkage in the model compounds. It can be concluded that this approach is potential for stabilizing the fragments and improving the yield of aromatic compounds from lignin.

The use of acid and/or high temperatures in lignin extraction process, as well as in the lignin depolymerization process, can lead to severe and irreversible condensation in the lignin structure. Most of the ether bonds in lignin are cleaved, and the stable carbon-carbon bonds are formed during the extraction process (Fig. 13A). Recently, Li *et al.*<sup>1,148</sup> attempted to prevent interunit carbon-carbon coupling during the extraction process by blocking the reactive benzylic positions with a protection reagent (Fig. 13B). It was reported that using formaldehyde to stabilize lignin could lead to the theoretical yield of aromatic monomers after hydrogenolysis of the extracted lignin. The production was about three to seven times higher than that obtained from extracted lignin without formaldehyde stabilization (Fig. 13). Formaldehyde played two roles in hindering the formation of C-C linkages: 1) in an acidic, water-deficient environment, formaldehyde can be converted to a stable six-membered 1,3-dioxane (acetal) structure with the 1,3-diols on lignin side-chains (Fig. 13B), blocking the formation of benzylic cations; 2) (protonated) formaldehyde substituted the

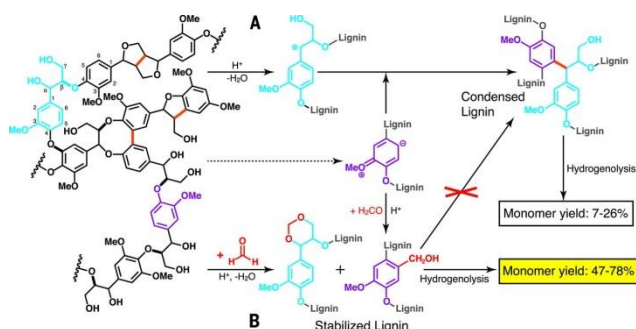


Fig. 13 Aromatic monomer production by lignin extraction followed by hydrogenolysis: (A) lignin extraction, condensation, and hydrogenolysis in a standard acidic process; (B) lignin extraction, stabilization with formaldehyde, and hydrogenolysis (Monomer yields, on a molar basis, are based on native Klason lignin), adapted from 148.

electron-rich positions at the *ortho* or *para* position to methoxyl groups on the aromatic ring to form hydroxymethyl groups (Fig. 13B). This method represents an outstanding advance in lignin upgrading process and will facilitate the development of other novel lignin extraction and depolymerization methodologies in the future.<sup>1</sup>

## 6 Conclusions

The conversion of lignins to renewable aromatic chemicals can not only meet the petroleum-based industry demand but also allow an effective and value-added disposal of lignin residues. Hydrogenolysis of lignin in solvent systems is attracting more and more attentions for producing aromatic platform chemicals, involving the effect of reaction conditions, solvent species and catalysts. Two-step LDP is proposed for enhancing the production of aromatic compounds and avoiding the repolymerization of the produced fragments. Considering the uncertainties of lignin hydrogenolysis mechanism and the limitations of its application, several issues should be addressed:

- (1) Development of moderate conditions for LHP (lignin hydrogenolysis process) (less energy input and H<sub>2</sub> consumption);
- (2) Technology for identifying the oligomers from LHP in order to address the inherent (catalytic) hydrogenolysis mechanism of lignin including the depolymerization and recondensation reactions;
- (3) Novel pretreatment method of lignin for suppressing the repolymerization of the produced fragments;
- (4) Design of an effective green catalyst promoting the cleavage of C-C and C-O bonds, giving selective production of target compounds, and improving the hydrothermal stability of the catalyst during LHP;
- (5) Low-cost separation technology of the specific aromatic compounds from the solvent system.

## Conflicts of interest

There are no conflicts to declare.

## Acknowledgements

The authors greatly acknowledge the funding support from the projects supported by National Natural Science Foundation of China (Grant Nos. 51676034 and 51628601), Natural Science Foundation of Jiangsu Province (project reference: BK20161423). This work is also supported by the Fundamental Research Funds for the Central Universities and Postgraduate Research & Practice Innovation Program of Jiangsu Province (project reference: KYCX17\_0074).

## Notes and references

- 1 M. D. Karkas, *ChemSusChem*, 2017, **10**, 2111-2115.
- 2 J. L. Sawin and F. Sverrisson, *Renewables 2014: Global status report*, REN21 Secretariat, Paris, 2014.
- 3 C. Li, X. Zhao, A. Wang, G. W. Huber and T. Zhang, *Chem. Rev.*, 2015, **115**, 11559-11624.
- 4 J. Zakzeski, P. C. A. Bruijninx, A. L. Jongerius and B. M. Weckhuysen, *Chem. Rev.*, 2010, **110**, 3552-3599.
- 5 F. G. Calvo-Flores and J. A. Dobado, *ChemSusChem*, 2010, **3**, 1227-1235.
- 6 H. Lange, S. Decina and C. Crestini, *Eur. Polym. J.*, 2013, **49**, 1151-1173.
- 7 G. W. Huber, S. Iborra and A. Corma, *Chem. Rev.*, 2006, **106**, 4044-4098.
- 8 J. A. Melero, J. Iglesias and A. Garcia, *Energ. Environ. Sci.*, 2012, **5**, 7393-7420.
- 9 P. Gallezot, *Chem. Soc. Rev.*, 2012, **41**, 1538-1558.
- 10 C. O. Tuck, E. Perez, I. T. Horvath, R. A. Sheldon and M. Poliakoff, *Science*, 2012, **337**, 695-699.
- 11 M. Besson, P. Gallezot and C. Pinel, *Chem. Rev.*, 2014, **114**, 1827-1870.
- 12 A. J. Ragauskas, G. T. Beckham, M. J. Bidy, R. Chandra, F. Chen, M. F. Davis, B. H. Davison, R. A. Dixon, P. Gilna, M. Keller, P. Langan, A. K. Naskar, J. N. Saddler, T. J. Tschaplinski, G. A. Tuskan and C. E. Wyman, *Science*, 2014, **344**, 709-721.
- 13 W. Boerjan, J. Ralph and M. Baucher, *Annual Review of Plant Biology*, 2003, **54**, 519-546.
- 14 R. A. Sheldon, *Green Chem.*, 2014, **16**, 950-963.
- 15 C. Cheng, J. Wang, D. Shen, J. Xue, S. Guan, S. Gu and K. Luo, *Polymers*, 2017, **9**, 240.
- 16 A. S. Mamman, J.-M. Lee, Y.-C. Kim, I. T. Hwang, N.-J. Park, Y. K. Hwang, J.-S. Chang and J.-S. Hwang, *Biofuels, Bioprod. Biorefin.*, 2008, **2**, 438-454.
- 17 W. O. S. Doherty, P. Mousavioun and C. M. Fellows, *Ind. Crops Prod.*, 2011, **33**, 259-276.
- 18 G. Zhu, X. Ouyang, Y. Yang, T. Ruan and X. Qiu, *RSC Adv.*, 2016, **6**, 17880-17887.
- 19 J. C. Serrano-Ruiz, R. Luque and A. Sepúlveda-Escribano, *Chem. Soc. Rev.*, 2011, **40**, 5266-5281.
- 20 R. Rinaldi, R. Palkovits and F. Schüth, *Angew. Chem., Int. Ed.*, 2008, **47**, 8047-8050.
- 21 G. W. Huber, J. N. Chheda, C. J. Barrett and J. A. Dumesic, *Science*, 2005, **308**, 1446-1450.
- 22 I. C. a. P. J. A. Gosselinka, E. d. Jonga, B. Guranb and A. Abächerlib, *Ind. Crops Prod.*, 2004, **20**, 121-129.
- 23 S. Farag, L. Kouisni and J. Chaouki, *Energ. Fuel.*, 2014, **28**, 1406-1417.
- 24 P. Azadi, O. R. Inderwildi, R. Farnood and D. A. King, *Renew.*

- Sustain. Energy Rev.*, 2013, **21**, 506-523.
- 25 J. Zakzeski, A. L. Jongerius, P. C. Bruijninx and B. M. Weckhuysen, *ChemSusChem*, 2012, **5**, 1602-1609.
- 26 S. N. Naik, V. V. Goud, P. K. Rout and A. K. Dalai, *Renew. Sustain. Energy Rev.*, 2010, **14**, 578-597.
- 27 L. H. Hu, H. Pan, Y. H. Zhou and M. Zhang, *BioResources*, 2011, **6**, 3515-3525.
- 28 J. Kong, B. Li and C. Zhao, *RSC Adv.*, 2016, **6**, 71940-71951.
- 29 P. J. Deuss and K. Barta, *Coordin. Chem. Rev.*, 2016, **306**, 510-532.
- 30 S. Kang, X. Li, J. Fan and J. Chang, *Renew. Sustain. Energy Rev.*, 2013, **27**, 546-558.
- 31 D. Carpenter, T. L. Westover, S. Czernik and W. Jablonski, *Green Chem.*, 2014, **16**, 384-406.
- 32 D. Shen, R. Xiao, S. Gu and K. Luo, *RSC Adv.*, 2011, **1**, 1641-1660.
- 33 D. Shen, W. Jin, J. Hu, R. Xiao and K. Luo, *Renew. Sustain. Energy Rev.*, 2015, **51**, 761-774.
- 34 T. Yokoyama, *J. Wood Chem. Technol.*, 2014, **35**, 27-42.
- 35 G. Chatel and R. D. Rogers, *ACS Sustain. Chem. Eng.*, 2014, **2**, 322-339.
- 36 R. Behling, S. Valange and G. Chatel, *Green Chem.*, 2016, **18**, 1839-1854.
- 37 C. Xu, R. A. D. Arancon, J. Labidid and R. Luque, *Chem. Soc. Rev.*, 2014, **43**, 7485-7500.
- 38 P. J. Deuss, K. Barta and J. G. de Vries, *Catal. Sci. Technol.*, 2014, **4**, 1174-1196.
- 39 C. Espro, B. Gumina, E. Paone and F. Mauriello, *Catalysts*, 2017, **7**, 78.
- 40 J. Pan, J. Fu, S. Deng and X. Lu, *Fuel Process. Technol.*, 2015, **140**, 262-266.
- 41 M. I. F. Mota, P. C. Rodrigues Pinto, J. M. Loureiro and A. E. Rodrigues, *Sep. Purif. Technol.*, 2015, **45**, 227-259.
- 42 R. Shmulsky and P. D. Jones, in *Forest Products and Wood Science An Introduction*, Wiley-Blackwell, 2011, DOI: 10.1002/9780470960035.ch3, pp. 45-63.
- 43 A. Brandt, J. Grasvik, J. P. Hallett and T. Welton, *Green Chem.*, 2013, **15**, 550-583.
- 44 S. Shimizu, T. Yokoyama, T. Akiyama and Y. Matsumoto, *Journal of Agricultural and Food Chemistry*, 2012, **60**, 6471-6476.
- 45 S. Gillet, M. Aguedo, L. Petitjean, A. R. C. Morais, A. M. da Costa Lopes, R. M. Łukasik and P. T. Anastas, *Green Chem.*, 2017, DOI: 10.1039/c7gc01479a.
- 46 D. Stewart, *Ind. Crops Prod.*, 2008, **27**, 202-207.
- 47 C. Crestini, M. Crucianelli, M. Orlandi and R. Saladino, *Catal. Today*, 2010, **156**, 8-22.
- 48 C. Dong, C. Feng, Q. Liu, D. Shen and R. Xiao, *Bioresour. Technol.*, 2014, **162**, 136-141.
- 49 D. Shen, N. Liu, C. Dong, R. Xiao and S. Gu, *Chem. Eng. J.*, 2015, **270**, 641-647.
- 50 H. Nimz, *Angew. Chem., Int. Ed.*, 1974, **13**, 313-321.
- 51 M. Erickson, S. Larsson and G. E. Miksche, *Acta Chem. Scand.*, 1973, **27**, 903-914.
- 52 R. Hage and A. Lienke, *Angew. Chem., Int. Ed.*, 2006, **45**, 206-222.
- 53 J. Hu, R. Xiao, D. Shen and H. Zhang, *Bioresour. Technol.*, 2013, **128**, 633-639.
- 54 C. Peng, Q. Chen, H. Guo, G. Hu, C. Li, J. Wen, H. Wang, T. Zhang, Z. K. Zhao, R. Sun and H. Xie, *ChemCatChem*, 2017, **9**, 1135-1143.
- 55 H. Wang, H. Ben, H. Ruan, L. Zhang, Y. Pu, M. Feng, A. J. Ragauskas and B. Yang, *ACS Sustain. Chem. Eng.*, 2017, **5**, 1824-1830.
- 56 Y. S. Choi, R. Singh, J. Zhang, G. Balasubramanian, M. R. Sturgeon, R. Katahira, G. Chupka, G. T. Beckham and B. H. Shanks, *Green Chem.*, 2016, **18**, 1762-1773.
- 57 W. G. Forsythe, M. D. Garrett, C. Hardacre, M. Nieuwenhuyzen and G. N. Sheldrake, *Green Chem.*, 2013, **15**, 3031-3038.
- 58 B. Sedai, C. Díaz-Urrutia, R. T. Baker, R. Wu, L. A. P. Silks and S. K. Hanson, *ACS Catal.*, 2013, **3**, 3111-3122.
- 59 G. V. B. Reddy, M. Sridhar and M. H. Gold, *Eur. J. Biochem.*, 2003, **270**, 284-292.
- 60 F. Tran, C. S. Lancefield, P. C. J. Kamer, T. Lebl and N. J. Westwood, *Green Chem.*, 2015, **17**, 244-249.
- 61 X.-P. Ouyang, C.-L. Liu, Y.-X. Pang and X.-Q. Qiu, *Chinese Chem. Lett.*, 2013, **24**, 1091-1094.
- 62 R. Behling, S. Valange and G. Chatel, *Green Chem.*, 2016, **18**, 1839-1854.
- 63 X. Ouyang, G. Zhu, X. Huang and X. Qiu, *J. Energ. Chem.*, 2015, **24**, 72-76.
- 64 A. G. Sergeev and J. F. Hartwig, *Science*, 2011, **332**, 439-443.
- 65 A. G. Sergeev, J. D. Webb and J. F. Hartwig, *J. Am. Chem. Soc.*, 2012, **134**, 20226-20229.
- 66 W. Xu, S. J. Miller, P. K. Agrawal and C. W. Jones, *ChemSusChem*, 2012, **5**, 667-675.
- 67 A. Kloekhorst, Y. Shen, Y. Yie, M. Fang and H. J. Heeres, *Biomass Bioenergy*, 2015, **80**, 147-161.
- 68 Y. Ye, Y. Zhang, J. Fan and J. Chang, *Bioresour. Technol.*, 2012, **118**, 648-651.
- 69 S. M. G. Lama, J. Pampel, T.-P. Fellinger, V. P. Beškoski, L. Slavković-Beškoski, M. Antonietti and V. Molinari, *ACS Sustain. Chem. Eng.*, 2017, **5**, 2415-2420.
- 70 Q. Song, F. Wang, J. Cai, Y. Wang, J. Zhang, W. Yu and J. Xu, *Energ. Environ. Sci.*, 2013, **6**, 994-1007.
- 71 X. Wang and R. Rinaldi, *ChemSusChem*, 2012, **5**, 1455-1466.
- 72 K. Barta, T. D. Matson, M. L. Fettig, S. L. Scott, A. V. Iretskii and P. C. Ford, *Green Chem.*, 2010, **12**, 1640-1647.
- 73 T. D. Matson, K. Barta, A. V. Iretskii and P. C. Ford, *J. Am. Chem. Soc.*, 2011, **133**, 14090-14097.
- 74 K. Barta, G. R. Warner, E. S. Beach and P. T. Anastas, *Green Chem.*, 2014, **16**, 191-196.
- 75 M. Chui, G. Metzker, C. M. Bernt, A. T. Tran, A. C. B. Burtoloso and P. C. Ford, *ACS Sustain. Chem. Eng.*, 2017, **5**, 3158-3169.
- 76 R. Ma, W. Hao, X. Ma, Y. Tian and Y. Li, *Angew. Chem., Int. Ed.*, 2014, **53**, 7310-7315.
- 77 F. Yan, R. Ma, X. Ma, K. Cui, K. Wu, M. Chen and Y. Li, *Appl. Catal. B: Environ.*, 2017, **202**, 305-313.
- 78 L. Chen, T. I. Koranyi and E. J. Hensen, *Chem. Commun.*, 2016, **52**, 9375-9378.
- 79 V. Molinari, C. Giordano, M. Antonietti and D. Esposito, *J. Am. Chem. Soc.*, 2014, **136**, 1758-1761.
- 80 J. Zhang, H. Asakura, J. van Rijn, J. Yang, P. Duchesne, B. Zhang, X. Chen, P. Zhang, M. Saeys and N. Yan, *Green Chem.*, 2014, **16**, 2432-2437.
- 81 J. Zhang, J. Teo, X. Chen, H. Asakura, T. Tanaka, K. Teramura and N. Yan, *ACS Catal.*, 2014, **4**, 1574-1583.
- 82 Y. Zhai, C. Li, G. Xu, Y. Ma, X. Liu and Y. Zhang, *Green Chem.*, 2017, **19**, 1895-1903.
- 83 Z. Tang, Y. Zhang and Q. Guo, *Ind. Eng. Chem. Res.*, 2010, **49**, 2040-2046.
- 84 M. Oregui Bengoechea, A. Hertzberg, N. Miletić, P. L. Arias and T. Barth, *J. Anal. Appl. Pyrol.*, 2015, **113**, 713-722.
- 85 A. Toledano, L. Serrano, A. Pineda, A. A. Romero, R. Luque and J. Labidi, *Appl. Catal. B: Environ.*, 2014, **145**, 43-55.
- 86 P. Chen, Q. Zhang, R. Shu, Y. Xu, L. Ma and T. Wang, *Bioresour. Technol.*, 2017, **226**, 125-131.
- 87 L. Liguori and T. Barth, *J. Anal. Appl. Pyrol.*, 2011, **92**, 477-484.
- 88 G. Yao, G. Wu, W. Dai, N. Guan and L. Li, *Fuel*, 2015, **150**,

- 175-183.
- 89 H. Wang, H. Ruan, M. Feng, Y. Qin, H. Job, L. Luo, C. Wang, M. H. Engelhard, E. Kuhn, X. Chen, M. P. Tucker and B. Yang, *ChemSusChem*, 2017, **10**, 1846-1856.
- 90 D. D. Laskar, M. P. Tucker, X. Chen, G. L. Helms and B. Yang, *Green Chem.*, 2014, **16**, 897-910.
- 91 R. Shu, Q. Zhang, L. Ma, Y. Xu, P. Chen, C. Wang and T. Wang, *Bioresour Technol*, 2016, **221**, 568-575.
- 92 C. Li, M. Zheng, A. Wang and T. Zhang, *Energ. Environ. Sci.*, 2012, **5**, 6383-6390.
- 93 X. Ma, Y. Tian, W. Hao, R. Ma and Y. Li, *Appl. Catal. A: Gen.*, 2014, **481**, 64-70.
- 94 A. L. Jongerius, P. C. A. Bruijninx and B. M. Weckhuysen, *Green Chem.*, 2013, **15**, 3049-3056.
- 95 J. Sun, T. Dutta, R. Parthasarathi, K. H. Kim, N. Tolic, R. K. Chu, N. G. Isern, J. R. Cort, B. A. Simmons and S. Singh, *Green Chem.*, 2016, **18**, 6012-6020.
- 96 H. Yoshida, Y. Onodera, S.-i. Fujita, H. Kawamori and M. Arai, *Green Chem.*, 2015, **17**, 1877-1883.
- 97 A. Toledano, L. Serrano, J. Labidi, A. Pineda, A. M. Balu and R. Luque, *ChemCatChem*, 2013, **5**, 977-985.
- 98 A. Toledano, L. Serrano, A. M. Balu, R. Luque, A. Pineda and J. Labidi, *ChemSusChem*, 2013, **6**, 529-536.
- 99 N. M. Bertero, A. F. Trasarti, C. R. Apesteguia and A. J. Marchi, *Appl. Catal. A: Gen.*, 2011, **394**, 228-238.
- 100 S. Cheng, C. Wilks, Z. Yuan, M. Leitch and C. Xu, *Polymer Degradation and Stability*, 2012, **97**, 839-848.
- 101 M. Oregui-Bengoechea, I. Gandarias, P. L. Arias and T. Barth, *ChemSusChem*, 2017, **10**, 754-766.
- 102 J. A. Barrett, Y. Gao, C. M. Bernt, M. Chui, A. T. Tran, M. B. Foston and P. C. Ford, *ACS Sustain. Chem. Eng.*, 2016, **4**, 6877-6886.
- 103 J. Zakzeski and B. M. Weckhuysen, *ChemSusChem*, 2011, **4**, 369-378.
- 104 X. Ouyang, X. Huang, Y. Zhu and X. Qiu, *Energ. Fuel.*, 2015, **29**, 5835-5840.
- 105 R. J. Gosselink, W. Teunissen, J. E. van Dam, E. de Jong, G. Gellerstedt, E. L. Scott and J. P. Sanders, *Bioresour Technol*, 2012, **106**, 173-177.
- 106 J. Tsujino, H. Kawamoto and S. Saka, *Wood Science and Technology*, 2003, **37**, 299-307.
- 107 T. Nimmanwudipong, R. C. Runnebaum, D. E. Block and B. C. Gates, *Energ. Fuel.*, 2011, **25**, 3417-3427.
- 108 T. H. Parsell, B. C. Owen, I. Klein, T. M. Jarrell, C. L. Marcum, L. J. Hauptert, L. M. Amundson, H. I. Kenttämaa, F. Ribeiro, J. T. Miller and M. M. Abu-Omar, *Chem. Sci.*, 2013, **4**, 806-813.
- 109 S. Huang, N. Mahmood, M. Tymchyshyn, Z. Yuan and C. Xu, *Bioresour. Technol.*, 2014, **171**, 95-102.
- 110 J. Hu, D. Shen, S. Wu, H. Zhang and R. Xiao, *Energ. Fuel.*, 2014, **28**, 4260-4266.
- 111 A. F. Trasarti, N. M. Bertero, C. R. Apesteguia and A. J. Marchi, *Appl. Catal. A: Gen.*, 2014, **475**, 282-291.
- 112 B. Güvenatam, O. Kurşun, E. H. J. Heeres, E. A. Pidko and E. J. M. Hensen, *Catal. Today*, 2014, **233**, 83-91.
- 113 W. Song, Y. Liu, E. Baráth, C. Zhao and J. A. Lercher, *Green Chem.*, 2015, **17**, 1204-1218.
- 114 C. Zhao, S. Kasakov, J. He and J. A. Lercher, *J. Catal.*, 2012, **296**, 12-23.
- 115 X. Wang and R. Rinaldi, *Angew. Chem., Int. Ed.*, 2013, **52**, 11499-11503.
- 116 H. Ohta, H. Kobayashi, K. Hara and A. Fukuoka, *Chem. Commun.*, 2011, **47**, 12209-12211.
- 117 H. Ohta, B. Feng, H. Kobayashi, K. Hara and A. Fukuoka, *Catal. Today*, 2014, **234**, 139-144.
- 118 I. Tyrone Ghampson, C. Sepúlveda, R. Garcia, J. L. García Fierro, N. Escalona and W. J. DeSisto, *Appl. Catal. A: Gen.*, 2012, **435-436**, 51-60.
- 119 A. L. Jongerius, R. Jastrzebski, P. C. A. Bruijninx and B. M. Weckhuysen, *J. Catal.*, 2012, **285**, 315-323.
- 120 Y.-C. Lin, C.-L. Li, H.-P. Wan, H.-T. Lee and C.-F. Liu, *Energ. Fuel.*, 2011, **25**, 890-896.
- 121 A. L. Jongerius, R. W. Gosselink, J. Dijkstra, J. H. Bitter, P. C. A. Bruijninx and B. M. Weckhuysen, *ChemCatChem*, 2013, **5**, 2964-2972.
- 122 M. Kim, J.-M. Ha, K.-Y. Lee and J. Jae, *Catal. Commun.*, 2016, **86**, 113-118.
- 123 C. R. Lee, J. S. Yoon, Y.-W. Suh, J.-W. Choi, J.-M. Ha, D. J. Suh and Y.-K. Park, *Catal. Commun.*, 2012, **17**, 54-58.
- 124 R. Shu, Y. Xu, L. Ma, Q. Zhang, P. Chen and T. Wang, *Catal. Commun.*, 2017, **91**, 1-5.
- 125 J. Long, S. Shu, Q. Wu, Z. Yuan, T. Wang, Y. Xu, X. Zhang, Q. Zhang and L. Ma, *Energ. Convers. Manage.*, 2015, **105**, 570-577.
- 126 H. Fang, J. Zheng, X. Luo, J. Du, A. Roldan, S. Leoni and Y. Yuan, *Appl. Catal. A: Gen.*, 2017, **529**, 20-31.
- 127 C. Zhao and J. A. Lercher, *ChemCatChem*, 2012, **4**, 64-68.
- 128 X. Cui, H. Yuan, K. Junge, C. Topf, M. Beller and F. Shi, *Green Chem.*, 2017, **19**, 305-310.
- 129 M. Chatterjee, A. Chatterjee, T. Ishizaka and H. Kawanami, *Catal. Sci. Technol.*, 2015, **5**, 1532-1539.
- 130 M. Wang, H. Shi, D. M. Camaioni and J. A. Lercher, *Angewandte. Chemie.*, 2017, **56**, 2110-2114.
- 131 J. He, C. Zhao and J. A. Lercher, *J. Am. Chem. Soc.*, 2012, **134**, 20768-20775.
- 132 J.-w. Zhang, Y. Cai, G.-p. Lu and C. Cai, *Green Chem.*, 2016, **18**, 6229-6235.
- 133 G. Zhu, X. Ouyang, L. Jiang, Y. Zhu, D. Jin, Y. Pang and X. Qiu, *Fuel Process. Technol.*, 2016, **154**, 132-138.
- 134 R. Zhu, B. Wang, M. Cui, J. Deng, X. Li, Y. Ma and Y. Fu, *Green Chem.*, 2016, **18**, 2029-2036.
- 135 M. Dawange, M. V. Galkin and J. S. M. Samec, *ChemCatChem*, 2015, **7**, 401-404.
- 136 A. Rahimi, A. Ulbrich, J. J. Coon and S. S. Stahl, *Nature*, 2014, **515**, 249-252.
- 137 P. C. A. Bruijninx and B. M. Weckhuysen, *Nat. Chem.*, 2014, **6**, 1035-1036.
- 138 A. Rahimi, A. Azarpira, H. Kim, J. Ralph and S. S. Stahl, *J. Am. Chem. Soc.*, 2013, **135**, 6415-6418.
- 139 C. S. Lancefield, O. S. Ojo, F. Tran and N. J. Westwood, *Angew. Chem., Int. Ed.*, 2015, **54**, 258-262.
- 140 Z. Jiang, T. He, J. Li and C. Hu, *Green Chem.*, 2014, **16**, 4257-4265.
- 141 J. Hu, D. Shen, S. Wu, H. Zhang and R. Xiao, *RSC Adv.*, 2015, **5**, 43972-43977.
- 142 W. Xiao, L. Han and Y. Zhao, *Ind. Crops Prod.*, 2011, **34**, 1602-1606.
- 143 A. Sequeiros, L. Serrano, R. Briones and J. Labidi, *J. Appl. Polym. Sci.*, 2013, **130**, 3292-3298.
- 144 A. Toledano, L. Serrano and J. Labidi, *Fuel*, 2014, **116**, 617-624.
- 145 P. J. Deuss, M. Scott, F. Tran, N. J. Westwood, J. G. de Vries and K. Barta, *J. Am. Chem. Soc.*, 2015, **137**, 7456-7467.
- 146 P. J. Deuss, C. W. Lahive, C. S. Lancefield, N. J. Westwood, P. C. Kamer, K. Barta and J. G. de Vries, *ChemSusChem*, 2016, **9**, 2974-2981.
- 147 C. W. Lahive, P. J. Deuss, C. S. Lancefield, Z. Sun, D. B. Cordes, C. M. Young, F. Tran, A. M. Slawin, J. G. de Vries, P. C. Kamer, N. J. Westwood and K. Barta, *J Am Chem Soc*, 2016, **138**, 8900-8911.
- 148 L. Shuai, M. T. Amiri, Y. M. Questell-Santiago, F. Héroguel, Y. Li, H. Kim, R. Meilan, C. Chapple, J. Ralph and J. S.

Luterbacher, *Science*, 2016, **354**, 329-333.